
Conditionally valid Probabilistic Conformal Prediction

Vincent Plassier¹ Alexander Fishkov^{2,4} Maxim Panov² Eric Moulines^{2,3}

¹ Lagrange Mathematics and Computing Research Center

² Mohamed bin Zayed University of Artificial Intelligence

³ CMAP, Ecole Polytechnique

⁴ Skolkovo Institute of Science and Technology
vincent.plassier@ens-paris-saclay.fr

Abstract

We develop a new method for creating prediction sets that combines the flexibility of conformal methods with an estimate of the conditional distribution $P_{Y|X}$. Most existing methods, such as conformalized quantile regression and probabilistic conformal prediction, only offer marginal coverage guarantees. Our approach extends these methods to achieve conditional coverage, which is essential for many practical applications. While exact conditional guarantees are impossible without assumptions about the data distribution, we provide non-asymptotic bounds that explicitly depend on the quality of the available estimate of the conditional distribution. Our confidence sets are highly adaptive to the local structure of the data, making them particularly useful in high heteroskedasticity situations. We demonstrate the effectiveness of our approach through extensive simulations, showing that it outperforms existing methods in terms of conditional coverage and improves the reliability of statistical inference in a wide range of applications.

1 Introduction

Conformal predictions are commonly used to construct prediction sets. Under minimal assumptions, they offer finite-sample validity [40, 36]. However, significant challenges arise with high heteroskedasticity, often leading to incorrect inferences [11].

The split-conformal approach uses a set of n calibration data points $\{(X_k, Y_k)\}_{k \in [n]}$ with $X_k \in \mathbb{R}^d$ and $Y_k \in \mathcal{Y}$ to create a prediction set $\mathcal{C}_\alpha(x)$ where $\alpha \in (0, 1)$. For each $x \in \mathbb{R}^d$, the prediction set based on a conformity score function $V: \mathbb{R}^d \times \mathcal{Y} \rightarrow \mathbb{R}$, is given by

$$\mathcal{C}_\alpha(x) = \left\{ y \in \mathcal{Y}: V(x, y) \leq Q_{1-\alpha} \left(\frac{1}{n+1} \sum_{k=1}^n \delta_{V(X_k, Y_k)} + \frac{1}{n+1} \delta_\infty \right) \right\},$$

where $Q_{1-\alpha}$ represents $(1 - \alpha)$ -quantile of the adjusted empirical score distribution $\frac{1}{n+1} \sum_{k=1}^n \delta_{V(X_k, Y_k)} + \frac{1}{n+1} \delta_\infty$. If the calibrations data $\{(X_k, Y_k)\}_{k \in [n]}$ are drawn i.i.d. from a population distribution $P_{X, Y}$, then for any new data point $(X_{n+1}, Y_{n+1}) \sim P_{X, Y}$ sampled independently of the calibration data, the conformal theory ensures the *marginal validity* of $\mathcal{C}_\alpha(X_{n+1})$, meaning that

$$\mathbb{P}(Y_{n+1} \in \mathcal{C}_\alpha(X_{n+1})) \geq 1 - \alpha.$$

Initially, most of the conformal methods focused on estimating a mean regression function for $Y | X$, to then construct a fixed-width band around it; see [39, 40]. However, as pointed out by [21], this marginal guarantee can hide significant discrepancies in the coverage of different regions of the input space \mathbb{R}^d . In particular, certain regions may be over-covered while others are under-covered. To solve this problem, it is necessary to construct adaptive prediction sets. Conditional conformal prediction

methods allow the generation of confidence intervals that adapt to the test point under consideration X_{n+1} . For example, if a patient has certain characteristics, the goal is to guarantee that their treatment will be successful with a confidence of $1 - \alpha$. Therefore, we want to adapt the guarantees to the profile of the individual instead of giving guarantees that only apply to the population as a whole. In particular, for any point $x \in \mathbb{R}^d$, the set $\mathcal{C}_\alpha(x)$ is described as *conditional valid* if

$$\mathbb{P}(Y_{n+1} \in \mathcal{C}_\alpha(X_{n+1}) \mid X_{n+1} = x) \geq 1 - \alpha.$$

Although conditional validity is a more desirable guarantee than marginal validity, it is difficult to achieve in practice without further assumptions about the data distribution. Indeed, it has been shown to be incompatible with the distribution-free setting [38, 25]. For practical purposes, however, an approximate conditional validity may be sufficient.

In regions with high heteroskedasticity, additional flexibility in the construction of prediction sets is useful. Methods based on quantile regression approaches were investigated in [30, 22]. These algorithms estimate the lower and upper conditional quantile regression functions $\hat{q}_{\alpha/2}$ and $\hat{q}_{1-\alpha/2}$; see e.g. [23, 2]. In [30], conditional confidence sets for $Y_{n+1} \mid X_{n+1}$ are constructed on the basis of the conformity assessment, which is determined by

$$V(x, y) = \max \{ \hat{q}_{\alpha/2}(x) - y, y - \hat{q}_{1-\alpha/2}(x) \}.$$

Then, denoting by $\mu = \frac{1}{n} \sum_{k=1}^n \delta_{V(X_k, Y_k)}$; the prediction set is defined as

$$\mathcal{C}_\alpha(x) = [\hat{q}_{\alpha/2}(X) - Q_{(1-\alpha)(1+n^{-1})}(\mu), \hat{q}_{1-\alpha/2}(X) + Q_{(1-\alpha)(1+n^{-1})}(\mu)],$$

where $Q_{(1-\alpha)(1+n^{-1})}(\mu)$ is the $(1 - \alpha)(1 + n^{-1})$ quantile of the distribution of μ . Possible improvements of this conformity score are also investigated in [22, 34]. In particular, [34] has shown that the constructed interval converges to the narrowest possible bands that achieve conditional coverage under mild assumptions. However, when the conditional distribution of the response has widely separated high-density regions, the ideal prediction set is not necessarily an interval. In such cases, a conformal method should be able to generate disjoint regions instead of being restricted to intervals; see Figure 1 for a simple illustration and [41] for a discussion and examples.

This paper is concerned with improving the construction of prediction sets, especially when an estimate of the conditional distribution $P_{Y \mid X}$ is available. The approach we propose utilizes the flexibility of conformal prediction methods to generate confidence sets that better capture the structure of the predictive distribution. This leads to improved conditional coverage and efficiency, especially in situations with high heteroskedasticity where the width of the confidence interval can vary significantly between regions.

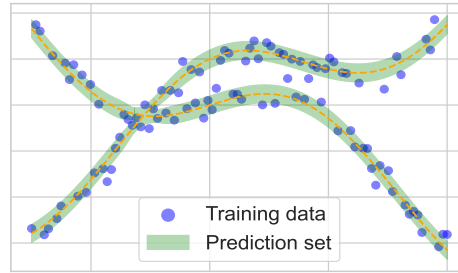


Figure 1: Bimodal example.

In order to achieve this, we pursue the fundamental question of how conditionally valid prediction sets can be derived. There are many, mostly negative, results on conditional validity, which can only be achieved under strong assumptions on the joint distribution of (X, Y) , which often fail to be satisfied [13]. One possible solution is to divide the space \mathbb{R}^d into several regions and learn a specific quantile for each of these regions [15, 16, 1]. However, this approach has significant drawbacks, especially since splitting the space \mathbb{R}^d into multiple regions for a given calibration set typically leads to an increase in the length of the prediction set [29, 27]. As shown in [3, 28], the conditional coverage follows a beta distribution. The error deviation is therefore of the order of $1/\sqrt{n_x}$, where n_x is the number of calibration data contained in the bin associated with x . Thus, an accuracy of 0.01 would require almost 10^4 data points in each bin, which limits the feasibility of binning methods.

Our proposed method aims to overcome these limitations and provide a more feasible and efficient solution for marginally valid prediction sets equipped with some conditional guarantees. In particular, our work addresses these challenges through the following main contributions:

- We propose a new method for constructing conditional confidence intervals that adapts to the local structure of the data distribution and allows the generation of confidence intervals that are more informative; see Section 2.

- We develop a theoretical framework to analyze the properties of the proposed method, establishing its approximate conditional validity; see Section 3.
- We demonstrate the effectiveness of the proposed method through a series of experiments on synthetic and real-world datasets; see Section 4. The results show that it outperforms existing methods in terms of conditional coverage.

2 Conditionally valid Probabilistic Conformal Prediction

Problem Setup and Sketch of the Method.

Suppose we are given n samples $\{(X_k, Y_k)\}_{k=1}^n$ and we must now predict the unknown value of Y_{n+1} at a test point X_{n+1} . We assume that all samples $\{(X_k, Y_k)\}_{k=1}^{n+1}$ are i.i.d. from an arbitrary joint distribution $\mathbb{P}_{X,Y}$ over the feature vectors $X \in \mathbb{R}^d$ and response variables $Y \in \mathcal{Y}$. The target set \mathcal{Y} can be either finite or continuous. Our goal is to construct a prediction set $\mathcal{C}_\alpha(X_{n+1})$ that contains the unobserved output Y_{n+1} with probability close to $1 - \alpha$, where $\alpha \in (0, 1)$ is the user-specified confidence level.

We aim to develop a flexible plug-and-play method that combines existing conformal methods with conditional distribution estimation $\mathbb{P}_{Y|X}$. We want to construct marginally valid predictive sets with approximate conditional validity. There are three main ingredients for our approach:

1. We specify a family of confidence sets $\mathcal{R}(x; t)$ parameterized by $t \in \mathbb{R}$. For instance, t can be chosen as the radius of a ball centered around an estimate of conditional mean $\mathbb{P}_{Y|X}$.
2. We split the available data into the training and calibration ones. An estimator $\Pi_{Y|X}$ of the conditional probability $\mathbb{P}_{Y|X}$ is learnt using the training data; see Remark 2.2. Given $x \in \mathbb{R}^d$, if $\Pi_{Y|X=x}$ closely approximates the true conditional probability $\mathbb{P}_{Y|X=x}$, then for any $\tau_x \in \mathbb{R}$ such that $\Pi_{Y|X=x}(\mathcal{R}(x; \tau_x)) \geq 1 - \alpha$, it follows that $\mathcal{R}(x; \tau_x)$ is an approximately valid prediction set; see Theorem 3.2 for more details.
3. We introduce $\lambda_{x,y} = \inf \{t \in \mathbb{R} : y \in \mathcal{R}(x; t)\}$, which can be considered as a conformity score for the input x and the observation y . On the calibration dataset, we determine τ_x using the model $\Pi_{Y|X}$; see details later in (3). We also introduce an increasing function $f_\tau(\lambda)$ parameterized by $\tau > 0$. An example of such a function is $f_\tau(\lambda) = \tau\lambda$. We then calculate the empirical measure μ of the transformed conformity values $f_{\tau X_k}^{-1}(\lambda_{X_k, Y_k})$. Finally, we determine the quantile $Q_{1-\alpha}(\mu)$ and construct the prediction set as follows

$$\mathcal{C}_\alpha(X_{n+1}) = \mathcal{R}\left(X_{n+1}; f_{\tau X_{n+1}}(Q_{1-\alpha}(\mu))\right), \quad (1)$$

which achieves marginal validity $\mathbb{P}(Y_{n+1} \in \mathcal{C}_\alpha(X_{n+1})) \geq 1 - \alpha$, see Theorem 3.1.

Remark 2.1. Conformal prediction methods are based on a conformity score $V(x, y)$, which evaluates how well the model prediction matches y . Given V , one can construct a family of confidence intervals $\mathcal{R}(x, t) = \{y \in \mathcal{Y} : V(x, y) \leq t\}$. With this definition, $\lambda_{x,y} = V(x, y)$; therefore, $\lambda_{x,y}$ plays the role of conformity measure. In (1), if we take $f_\tau(\lambda) = \lambda$, the standard conformal method is used. On the other hand, if we set $f_\tau(\lambda) = \tau$, then the confidence set is completely determined by the conditional generative model (we trust our conditional distribution but lose conformal guarantees). Taking $f_{\tau X_{n+1}}(Q_{1-\alpha}(\mu))$ provides a compromise between the “simple” conformal method $Q_{1-\alpha}(\mu)$ and the confidence set derived from the conditional distribution, expressed by τ_x . In this context, $\tilde{V}(x, y) = f_{\tau_x}^{-1}(\lambda_{x,y})$ can be viewed as an “adjusted” conformity measure. Consequently, (1) represents the conformal prediction set derived from the conformity score function \tilde{V} . This relationship directly establishes the finite sample marginal validity.

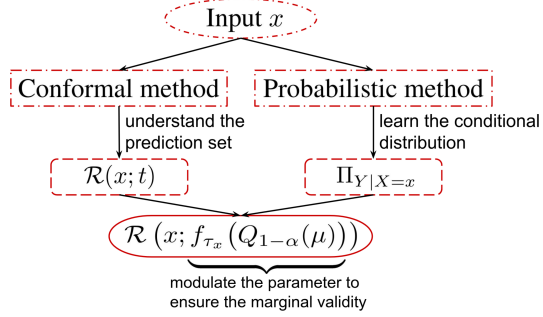


Figure 2: Schematic representation of CP².

Remark 2.2. If the predictive distribution has multiple modes, a single interval centered around the predictive mean often fails to provide an informative prediction set. Ideally, $\mathcal{R}(x; t)$ should correspond to the intervals with the highest probability density (HPD) of $P_{Y|X}$; HPD regions are difficult to determine in practice, even when the conditional predictive density is available. [41] proposes a way to approximate HPD domains by using implicit conditional generative models. In this case, the prediction sets $\mathcal{R}_z(x; t)$ can depend on an exogenous variables $z \in \mathcal{Z}$, such as a union of balls with radius t centered at points sampled from $\Pi_{Y|X}$.

2.1 The CP² framework

We will now present our method for constructing adaptive prediction sets defined in (1). These sets are based on confidence set $\mathcal{R}_z(x; t)$ satisfying the following assumption.

H1. For all $(x, z) \in \mathbb{R}^d \times \mathcal{Z}$, the confidence sets $\{\mathcal{R}_z(x; t)\}_{t \in \mathbb{R}}$ are non-decreasing, and $\bigcap_{t \in \mathbb{R}} \mathcal{R}_z(x; t) = \emptyset$, $\bigcup_{t \in \mathbb{R}} \mathcal{R}_z(x; t) = \mathcal{Y}$, $\bigcap_{t' > t} \mathcal{R}_z(x; t') = \mathcal{R}_z(x; t)$.

In simpler terms, the size of $\mathcal{R}_z(x; t)$ grows with t . If we select a large enough value for t , we can cover the entire output space \mathcal{Y} . Let's introduce the parameter $\lambda_{x,y,z}$ which corresponds to the minimal radius needed to guarantee that the confidence set contains the output value y

$$\lambda_{x,y,z} = \inf \{t \in \mathbb{R} : y \in \mathcal{R}_z(x; t)\}. \quad (2)$$

Lemma 2.3. Assume **H1** holds. For any $(x, y, z) \in \mathbb{R}^d \times \mathcal{Y} \times \mathcal{Z}$, $\lambda_{x,y,z} \in (-\infty, +\infty)$ and $y \in \mathcal{R}_z(x; \lambda_{x,y,z})$.

Our method relies on a family of transformations, denoted as $\{\lambda \mapsto f_\tau(\lambda)\}_{\tau \in \mathbb{R}}$, which balance the following two factors:

- The optimal parameter $\lambda_{x,y,z}$ that ensures y is included in the confidence set $\mathcal{R}_z(x; \lambda_{x,y,z})$.
- The parameter $\tau_{x,z}$ obtained from the probabilistic model $\Pi_{Y|X=x}$.

H2. There exists $\varphi \in \mathbb{R}$ such that $\tau \in \mathbb{R} \mapsto f_\tau(\varphi)$ is increasing and bijective. Additionally, the function $\lambda \in \mathbb{R} \cup \{\infty\} \mapsto f_{\tau_{x,z}}(\lambda)$ is increasing for any $x \in \mathbb{R}^d$, $z \in \mathcal{Z}$, where $\tau_{x,z}$ is defined in (3).

Given the significance level $\alpha \in [0, 1]$, consider

$$\tau_{x,z} = \inf \{\tau \in \mathbb{R} : \Pi_{Y|X=x}(\mathcal{R}_z(x; f_\tau(\varphi))) \geq 1 - \alpha\} \quad (3)$$

where by convention, we set $\inf \emptyset = -\infty$.

Lemma 2.4. Assume **H1-H2** hold, and let $\alpha \in (0, 1)$, $x \in \mathbb{R}^d$, $z \in \mathcal{Z}$. If $\Pi_{Y|X=x}$ is a probability measure, then $\tau_{x,z} \in (-\infty, \infty)$ and $\Pi_{Y|X=x}(\mathcal{R}_z(x; f_{\tau_{x,z}}(\varphi))) \geq 1 - \alpha$.

In words, $\tau_{x,z}$ ensures that the confidence set $\mathcal{R}_z(x; f_{\tau_{x,z}}(\varphi))$ is approximately conditionally valid when the distribution of Y given $X = x$ is well approximated by the probabilistic model $\Pi_{Y|X=x}$.

For notational simplicity, set $\bar{\tau}_k := \tau_{X_k, Z_k}$ and $\bar{\lambda}_k := \lambda_{X_k, Y_k, Z_k}$. Given $X_{n+1} \in \mathbb{R}^d$, we sample $Z_{n+1} \sim \Pi_{Z|X=X_{n+1}}$ and construct the resulting CP² prediction set as

$$\mathcal{C}_\alpha(X_{n+1}) = \mathcal{R}_{Z_{n+1}}(X_{n+1}; f_{\bar{\tau}_{n+1}}(Q_{1-\alpha}(\mu))), \quad (4)$$

where $Q_{1-\alpha}(\mu)$ is the $1 - \alpha$ quantile of the distribution μ is given by

$$\mu = \frac{1}{n+1} \sum_{k=1}^n \delta_{f_{\bar{\tau}_k}^{-1}(\bar{\lambda}_k)} + \frac{1}{n+1} \delta_\infty. \quad (5)$$

Now, let's explore two examples of the CP² framework.

2.2 CP² with Explicit Conditional Generative Model: CP²-HPD

We illustrate a specific instance of our framework, called CP²-HPD. We suggest using this approach when an approximate of the density function is known, denoted by $\gamma_{Y|X=x}$. The confidence set is defined as $\mathcal{R}(x; t) = \{y \in \mathcal{Y}: \gamma_{Y|X=x}(y) \geq t\}$. We omit the variable z from the notation, as we do not consider exogenous randomization in this case. The parameter τ_x is obtained by solving $\Pi_{Y|X=x}(\mathcal{R}(x; f_\tau(\varphi))) = 1 - \alpha$. We then compute $\lambda_{x,y} = \gamma_{Y|X=x}(y)$ and derive the prediction set as

$$\mathcal{C}_\alpha(x) = \{y \in \mathcal{Y}: \gamma_{Y|X=x}(y) \geq f_{\tau_x}(Q_{1-\alpha}(\mu))\}.$$

If we take $f_\tau(\lambda) = \lambda$ and $\varphi = 1$, the method shares similarity with the CD-split method, proposed in [20]. While CD-split uses $\lambda_{x,y} = \gamma_{Y|X=x}(y)$ as the conformity score, our method uses $f_{\tau_x}^{-1}(\lambda_{x,y})$, which incorporates the information from τ_x to modify $\gamma_{Y|X=x}(y)$. Additionally, CP²-HPD does not rely on binning, unlike the CD-split approach.

2.3 CP² with Implicit Conditional Generative Model: CP²-PCP

We also develop a second instance of the CP² algorithm, which is inspired by [41]. Unlike CP²-HPD, this approach does not require the conditional density. Instead, it is designed for cases where the conditional generative model (CGM) $\Pi_{Y|X}$ is implicit, meaning we cannot evaluate it pointwise while being able to sample from it. For each calibration point X_k , we draw M random variables $\{\hat{Y}_{k,i}\}_{i=1}^M$ from $\Pi_{Y|X=X_k}$. We denote $Z_k = (\hat{Y}_{k,1}, \dots, \hat{Y}_{k,M})$ and consider the confidence sets as the union of spheres centered around the sample points:

$$\mathcal{R}_{Z_k}(X_k; t) = \cup_{i=1}^M \mathbb{B}(\hat{Y}_{k,i}, t).$$

With such choice, we get $\bar{\lambda}_k = \min_{i=1}^M \|Y_k - \hat{Y}_{k,i}\|$. We then draw a second sample $\{\tilde{Y}_{k,j}\}_{j=1}^{\bar{M}}$, and compute $\bar{\tau}_k = \{\tau \in \mathbb{R}_+: \sum_{j=1}^{\bar{M}} \mathbb{1}_{\tilde{Y}_{k,j} \in \mathcal{R}_{Z_k}(X_k; f_\tau(\varphi))} \geq 1 - \alpha\}$. It can be verified that

$$\bar{\tau}_k = (\tau \mapsto f_\tau(\varphi))^{-1} \left\{ Q_{1-\alpha} \left(\frac{1}{\bar{M}} \sum_{j=1}^{\bar{M}} \delta_{\min_{i=1}^M \|\tilde{Y}_{j,k} - \hat{Y}_{k,i}\|} \right) \right\}.$$

Given a new input $X_{n+1} \in \mathbb{R}^d$, we sample $Z_{n+1} = (\hat{Y}_{n+1,1}, \dots, \hat{Y}_{n+1,M})$ and obtain prediction set as follows

$$\mathcal{C}_\alpha(X_{n+1}) = \left\{ y \in \mathcal{Y}: \min_{i=1}^M \|y - \hat{Y}_{n+1,i}\| \leq f_{\bar{\tau}_{n+1}}(Q_{1-\alpha}(\mu)) \right\},$$

where μ is given in (5). The CP²-PCP method employs the same confidence set $\mathcal{R}_z(x; t)$ as the one used by PCP. This method effectively captures multimodalities using balls centered at likely outputs $\hat{Y}_{n+1,i}$. Furthermore, the conformity scores used by PCP correspond to our $\lambda_{x,y,z}$. However, the key distinction between the two algorithms lies in the additional parameter $\tau_{x,z}$ for CP²-PCP, which requires the generation of a second random sample from $\Pi_{Y|X=x}$.

2.4 Asymptotic Validity of CP²

To gain insights, we informally discuss the asymptotic conditional validity of CP². We assume for simplicity that $\mathbb{P}_{Y|X} = \Pi_{Y|X}$, i.e., the predictive distribution is known. If **H1** and **H2** hold, then Lemma 2.3 shows that

$$\begin{aligned} \mathbb{P}(\lambda_{X,Y,Z} \leq f_{\tau_{X,Z}}(t) | X = x, Z = z) &= \mathbb{P}(Y \in \mathcal{R}_z(x; f_{\tau_{x,z}}(t)) | X = x, Z = z) \\ &= \Pi_{Y|X=x}(\mathcal{R}_z(x; f_{\tau_{x,z}}(t))). \end{aligned}$$

Note that $\Pi_{Y|X=x}(\mathcal{R}_z(x; f_{\tau_{x,z}}(t))) \geq 1 - \alpha$ if and only if $t \geq \varphi$, which implies that

$$\mathbb{P}(f_{\tau_{x,z}}^{-1}(\lambda_{X,Y,Z}) \leq t | X = x, Z = z) \geq 1 - \alpha \quad \text{if and only if} \quad t \geq \varphi. \quad (6)$$

From (6) we deduce that the $(1 - \alpha)$ -quantile of $f_{\tau_{X,Z}}^{-1}(\lambda_{X,Y,Z})$ is φ . The Glivenko–Cantelli Theorem [37, Theorem 19.1] demonstrates that $\sup_{t \in \mathbb{R}} |\mu(-\infty, t] - \mathbb{P}(f_{\tau_{X,Z}}^{-1}(\lambda_{X,Y,Z}) \leq t)| \rightarrow 0$

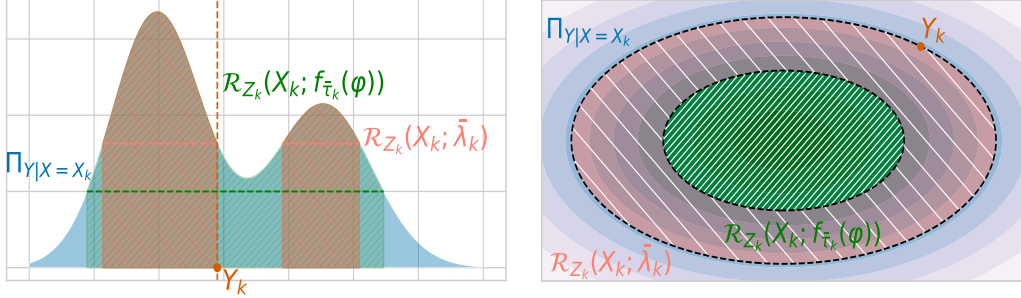


Figure 3: Examples of $\bar{\tau}_k$ and $\bar{\lambda}_k$ for two different scenarios. In both cases, $\bar{\tau}_k$ is selected such that the probability of the corresponding confidence set $\mathcal{R}_{Z_k}(X_k; \bar{f}_{\bar{\tau}_k}(\varphi))$ under the distribution $\Pi_{Y|X=X_k}$ is equal to $1 - \alpha$. On the other hand, $\bar{\lambda}_k$ is chosen as the smallest real number such that the true label Y_k belongs to the confidence set $\mathcal{R}_{Z_k}(X_k; \bar{\lambda}_k)$.

Table 1: Confidence sets $\mathcal{R}(x; t)$ found in the literature and also discussed in [18, Table 1].

[24]	[24]	[22]
$[\text{pred}(x) - t, \text{pred}(x) + t]$	$[\text{pred}(x) - t\sigma(x), \text{pred}(x) + t\sigma(x)]$	$(1 + t)[q_{\alpha/2}(x), q_{1-\alpha/2}(x)] - tq_{1/2}(x)$
[9]	[30]	[34]
$[q_t(x), q_{1-t}(x)]$	$[q_{\alpha/2}(x) - t, q_{1-\alpha/2}(x) + t]$	$[q_{\alpha/2}(x), q_{1-\alpha/2}(x)] \pm t(q_{1-\alpha/2}(x) - q_{\alpha/2}(x))$

almost surely as $n \rightarrow \infty$, where μ is defined in (5). Applying [37, Lemma 21.2], under weak conditions we deduce that $Q_{1-\alpha}(\mu) \rightarrow \varphi$ as $n \rightarrow \infty$.

If the quantile $Q_{1-\alpha}(\mu)$ is greater than φ , it indicates that there are insufficient calibration data points $Y_k \in \mathcal{R}_{Z_k}(X_k; \bar{f}_{\bar{\tau}_k}(\varphi))$. Conversely, if $Q_{1-\alpha}(\mu)$ is less than φ , it means that an excessive percentage of calibration data falls within the confidence set $\mathcal{R}_{Z_k}(X_k; \bar{f}_{\bar{\tau}_k}(\varphi))$. In this situation, the radius of the confidence set is increased to ensure the correct proportion of observations Y_k covered.

2.5 Related Work

Approximating the conditional distribution of $Y | X$ to construct prediction sets has been extensively studied. Methods based on density estimation, such as [6, 25], achieve asymptotic validity under appropriate conditions. [19] uses kernel density estimation to construct asymmetric prediction bands. However, this method cannot handle bimodality as it generates a single interval. On the other hand, [35] partitions the domain of Y into bins to create a histogram approximation of $P_{Y|X}$. The authors showed that their method satisfies the marginal validity while achieving the asymptotic conditional coverage. This property has also been derived in the context of regression [24]. Asymptotic conditional coverage is also obtained in [34, 8] using quantile regression-based methods, or using cumulative distribution function estimators [20, 9]. Conditionally valid prediction sets have been shown to improve the robustness to perturbations [14]. [41] introduced a method adapted to distributions with separated high-density regions and with implicit CGM. Recently, [17] converted regression problems into classification problems by binning the range space and discretizing the labels. They learn an approximation of the conditional density to generate prediction sets that match the HPD regions. Similarly, [12] proposed a method that estimates the conditional density using neural network parameterized splines. The concept of nested sets was investigated in the work of [18]. Additionally, [32] proposed an approach leading to a confidence set $\mathcal{R}(x; \tau) = [\hat{q}_{\text{lo}}(x, \tau), \hat{q}_{\text{hi}}(x, \tau)]$, where $\hat{q}_{\text{lo}}(x, \tau)$ and $\hat{q}_{\text{hi}}(x, \tau)$ are quantile regressors for the conditional distribution $Y | X$. Moreover, τ is set such that at least $100(1 - \alpha)\%$ of the calibration data fall within the prediction set.

3 Theoretical guarantees

In this section, we provide both marginal and conditional guarantees for the prediction set $\mathcal{C}_\alpha(x)$ given in (4). The validity of these guarantees is ensured by the exchangeability of the calibration data, with the exception of Corollary 3.3 which relies on a concentration inequality and thus requires that the calibration data are i.i.d. The following theorem establishes marginal validity of the predictive set defined by \mathcal{CP}^2 .

Theorem 3.1. *Assume **H1-H2**. Then, for any $\alpha \in (0, 1)$, it holds*

$$1 - \alpha \leq \mathbb{P}(Y_{n+1} \in \mathcal{C}_\alpha(X_{n+1})).$$

Moreover, if the conformity scores $\{f_{\bar{\tau}_k}^{-1}(\bar{\lambda}_k)\}_{k=1}^{n+1}$ are almost surely distinct, then it also holds that

$$\mathbb{P}(Y_{n+1} \in \mathcal{C}_\alpha(X_{n+1})) < 1 - \alpha + \frac{1}{n+1}.$$

The proof is postponed to Appendix A.1. Moreover, the upper bound on the coverage always holds when the distribution of $f_{\bar{\tau}_k}^{-1}(\bar{\lambda}_k)$ is continuous. Now, we will investigate the conditional validity of $\mathcal{C}_\alpha(x)$. Denote by d_{TV} the total variation distance.

Theorem 3.2. *Assume **H1-H2**, and let $\alpha \in (0, 1)$. For any $x \in \mathbb{R}^d$ and $z \in \mathcal{Z}$, it holds*

$$\mathbb{P}(Y_{n+1} \in \mathcal{C}_\alpha(x) \mid X_{n+1} = x, Z_{n+1} = z) \geq 1 - \alpha - d_{\text{TV}}(\mathbf{P}_{Y|X=x}; \Pi_{Y|X=x}) - p_{n+1}^{(x,z)},$$

where $p_{n+1}^{(x,z)} = \mathbb{P}(Q_{1-\alpha}(\mu) < f_{\bar{\tau}_{n+1}}^{-1}(\bar{\lambda}_{n+1}) \leq \varphi \mid X_{n+1} = x, Z_{n+1} = z)$.

The proof is postponed to Appendix A.1. The better the estimator $\Pi_{Y|X=x}$ is, the closer the result is to $1 - \alpha$. Achieving accurate conditional coverage at x does not require knowledge of the entire conditional distribution $\mathbf{P}_{Y|X}$. Instead, only a reliable approximation for the specific point x is required. The second term in the lower bound is $p_{n+1}^{(x,z)}$. Its expected value is upper bounded by $\mathbb{E}[p_{n+1}^{(x,z)}] \leq \alpha$, but analyzing this term is difficult. We address this problem in the following corollary, whose proof is postponed to Appendix A.2. Denote by F and \hat{F} the cumulative distribution functions of the random variables $f_{\tau_{X,Z}}^{-1}(\lambda_{X,Y,Z})$ and $f_{\tau_{X,\hat{Y},Z}}^{-1}(\lambda_{X,\hat{Y},Z})$, where $(X, Y, Z) \sim \mathbf{P}_X \otimes \mathbf{P}_{Y|X} \otimes \Pi_{Z|X}$ and $(X, \hat{Y}, Z) \sim \mathbf{P}_X \otimes \Pi_{Y|X} \otimes \Pi_{Z|X}$, respectively.

Corollary 3.3. *Assume **H1-H2**, and suppose the distribution of $f_{\tau_{X,Z}}^{-1}(\lambda_{X,Y,Z})$ is continuous. For any $x \in \mathbb{R}^d$, $z \in \mathcal{Z}$ and $\epsilon \in [0, 1 - \alpha)$, it holds that*

$$p_{n+1}^{(x,z)} \leq \exp(-n\Phi(\epsilon)) + \mathbb{P}\left(F^{-1}(1 - \alpha - \epsilon) < f_{\bar{\tau}_{n+1}}^{-1}(\bar{\lambda}_{n+1}) \leq \hat{F}^{-1}(1 - \alpha) \mid X_{n+1} = x, Z_{n+1} = z\right)$$

where $\Phi(\epsilon) = \epsilon[(u_\epsilon^{-1} - 1) \log(1 + u_\epsilon) - 1]$ and $u_\epsilon = \epsilon(\alpha + \epsilon)^{-1}(1 - \alpha - \epsilon)^{-1}$.

Setting $\epsilon = \sqrt{8\alpha(1 - \alpha)n^{-1} \log n}$ ensures that $\exp(-n\Phi(\epsilon)) \leq n^{-1}$. When F^{-1} is continuous, $F^{-1}(1 - \alpha)$ is approximately equal to $F^{-1}(1 - \alpha - \epsilon)$ for small ϵ . Therefore, if $\hat{F}^{-1}(1 - \alpha)$ closely approximates $F^{-1}(1 - \alpha)$, then Corollary 3.3 demonstrates that $p_{n+1}^{(x,z)}$ is always small.

The prediction set, defined in (4), is derived from the $(1 - \alpha)$ -quantile of the conformity scores $\{f_{\bar{\tau}_k}^{-1}(\bar{\lambda}_k)\}_{k=1}^n \cup \{\infty\}$. However, $\{\infty\}$ can be removed from these conformity scores. Inspired by [30, 34], the Corollary 3.4 ensures the marginal validity of

$$\bar{\mathcal{C}}_\alpha(x) = \mathcal{R}_z \left(x; f_{\tau_{x,z}} \left(Q_{(1-\alpha)(1+n^{-1})} \left(\frac{1}{n} \sum_{k=1}^n \delta_{f_{\bar{\tau}_k}^{-1}(\bar{\lambda}_k)} \right) \right) \right).$$

Corollary 3.4. *Under the same assumptions as in Theorem 3.1, for any $\alpha \in [1/(n+1), 1]$, we have*

$$1 - \alpha \leq \mathbb{P}(Y_{n+1} \in \bar{\mathcal{C}}_\alpha(X_{n+1})) < 1 - \alpha + \frac{1}{n+1},$$

where the upper bound only holds if the conformity scores $\{f_{\bar{\tau}_k}^{-1}(\bar{\lambda}_k)\}_{k=1}^{n+1}$ are almost surely distinct.

The proof of Corollary 3.4 is along the same lines as [41, Corollary 1]; see Appendix A.3.

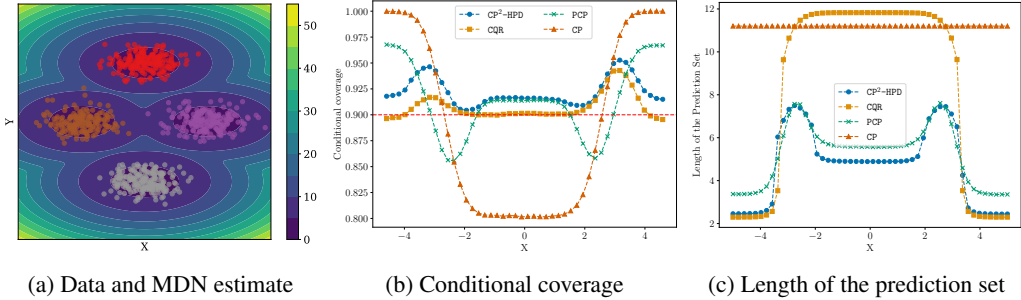


Figure 4: Mixture Density Network: the multimodal case.

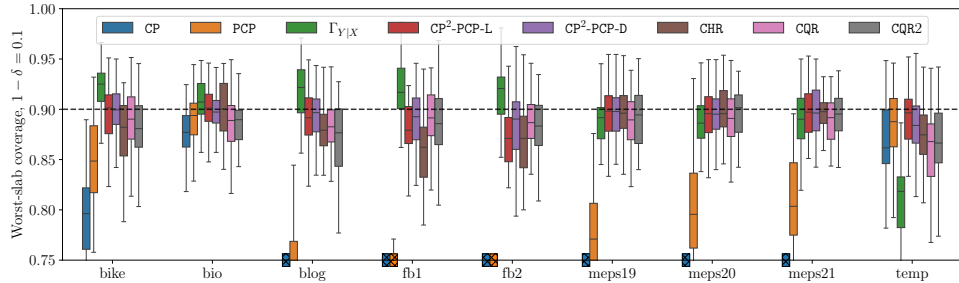


Figure 5: Worst-slab coverage on real data. Results averaged over 50 random splits of each dataset. Calibration and test set sizes set to 2000, 50 conditional samples for PCP, CP^2 and $\Pi_{Y|X}$. Worst-slab coverage parameter $(1 - \delta) = 0.1$. Nominal coverage level is $(1 - \alpha) = 0.9$ and is shown in dashed black. Methods with conditional coverage below 0.75 shown as cross-hatched on horizontal axis.

4 Numerical experiments

In this section, we conduct a comprehensive analysis demonstrating the advantage of CP^2 compared to standard and adaptive split conformal algorithms. Specifically, we benchmark our algorithm against two state-of-the-art methods: Conformalized Quantile Regression (CQR; [30]) and Probabilistic Conformal Prediction (PCP; [41]). We aim to answer these specific questions: how does CP^2 performs in terms of coverage, conditional coverage and predictive set volume when compared to state-of-the-art methods on synthetic and real data.

4.1 Synthetic data experiments

In this example, (X_k, Y_k) is sampled from a mixture of $P = 4$ Gaussians; see Figure 4a. The results for other classical 2-d datasets lead to similar conclusions. The number of training and calibration samples is $T = 10^4$ and $n = 10^3$, respectively. We fit a Mixture Density Network (MDN) as an explicit generative model, $\gamma_{Y|X=x}(y) = \sum_{\ell=1}^P \pi_{\ell}(x) \mathcal{N}(y; \mu_{\ell}(x), \sigma_{\ell}^2(x))$, where $\mu_{\ell}(\cdot)$, $\sigma_{\ell}(\cdot)$ and $\pi_{\ell}(\cdot)$ are all modeled by fully connected 2-layers neural networks (the condition $\sum_{\ell=1}^P \pi_{\ell}(x) = 1$ is ensured by using softmax activation functions). We use CP^2 -HPD (the calculation of the HPD rates as well as τ_x and $\lambda_{x,y}$ is explicit in this case). The parameters of the MDN are trained by maximizing the likelihood on the training set.

We compare the plain CP^2 -HPD, PCP (with the same MDN as CP^2 -HPD and $M = 50$ draws) and CQR. All methods achieve the desired nominal coverage $1 - \alpha = 0.9$. We illustrate the conditional coverage in Figure 4b and the lengths of the predictive sets in Figure 4c. CP^2 -HPD with a fixed-width predictive set performs poorly in this multimodal example, both in terms of the size of the confidence set and the conditional coverage. CP^2 -HPD and CQR perform similarly in terms of conditional coverage (which remains close to $1 - \alpha = 0.9$). The conditional coverage of PCP varies between 0.85 and 0.95. CP^2 produces shorter prediction sets compared to CQR and PCP. This is because CP^2 uses an HPD confidence set that is more suitable for multimodal applications than the confidence set used by CQR.

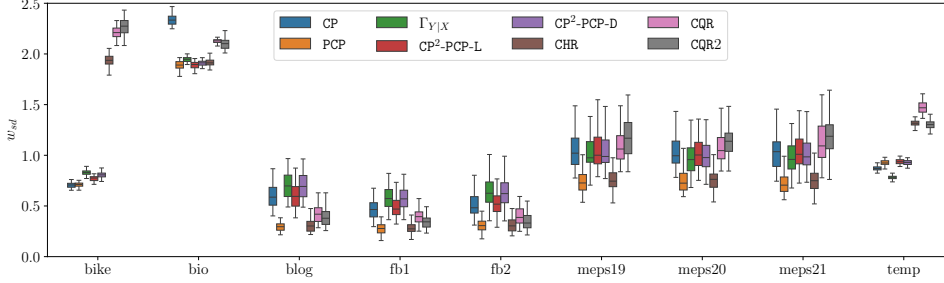


Figure 6: Sizes of the prediction sets on real data. We divide the size of the set by the standard deviation of response to present the results on the same scale.

4.2 Real data experiments

In this section, we study the performance of $\text{CP}^2\text{-PCP}$ on several real world regression datasets.

Datasets. We use publicly available regression datasets, which are also considered in [30, 41]. Some of them come from the UCI repository: bike sharing (`bike`), protein structure (`bio`), blog feedback (`blog`), Facebook comments (`fb1` and `fb2`). Other datasets come from US Department of Health surveys (`meps19`, `meps20` and `meps21`), and from weather forecasts (`temp`) [10].

Methods. We compare the proposed $\text{CP}^2\text{-PCP}$ method with Probabilistic Conformal Prediction (PCP; [41]), Conformalized Quantile Regression (CQR; [30]) and Conformalized Histogram Regression (CHR; [35]). We also consider CQR2 which is a modification of CQR that uses inverse quantile nonconformity score. For our method and PCP we use a Mixture Density Network [4] to estimate the conditional distribution $P_{Y|X}$, since it was chosen in [41] as best-performing. We also consider different choices of f_τ for our method: $\text{CP}^2\text{-PCP-L}$ stands for $\text{CP}^2\text{-PCP}$ with $f_\tau(\lambda) = \lambda\tau$ and $\text{CP}^2\text{-PCP-D}$ stands for $\text{CP}^2\text{-PCP}$ with $f_\tau(\lambda) = \lambda + \tau$. Our implementation of $\text{CP}^2\text{-PCP}$ is summarized in Algorithms 1 and 2. They use Brent’s method to find the optimal τ_x ; see (3). Additionally, we consider $\Pi_{Y|X}$ which is a special case of $\text{CP}^2\text{-PCP}$ with $f_\tau(\lambda) = \tau$.

Metrics. Empirical coverage (marginal and conditional) is the main quantity of interest for prediction sets. We evaluate worst-slab conditional coverage [8, 31] in our experiments, see details in Appendix B.3. We also measure the total size of the predicted sets, scaled by the standard deviation of the response Y .

Experimental setup. Our experimental setup closely follows [41]. We split each dataset into train, calibration and test portions and train a Mixture Density Network with 10 components to approximate $P_{Y|X}$. For each calibration and test point we first obtain the Gaussian Mixture parameters (this becomes $\Pi_{Y|X}$) and then sample $M = 5, 20, 50$ samples from these distributions (gives us $\mathcal{R}_z(x, \tau)$). We replicate this experiment on 50 different splits of each dataset.

Results of the experiments for $M = 50$ samples are presented in Figures 5 and 6, additional results are available in Appendix B. In terms of marginal coverage, all methods achieve the target $1 - \alpha$ value, except for $\Pi_{Y|X}$.

Standard conformal prediction fails to maintain the conditional coverage as expected. We can also observe that PCP consistently struggles with conditional coverage. On all the datasets $\text{CP}^2\text{-PCP}$ provides valid conditional coverage, while CQR fails on `blog` and `temp`. CHR method shows unstable performance not achieving conditional coverage more often than other methods but sometimes providing narrower predictions sets. Additionally, $\text{CP}^2\text{-PCP}$ significantly outperforms quantile regression-based methods in terms of size of the prediction sets on `bike`, `bio` and `temp` datasets.

Additionally, we assess conditional coverage with the help of clustering. We apply HDBSCAN [7, 26] method to cluster the test set and then compute coverage within clusters. Results for `fb1` dataset are presented in Figure 7. We again observe that CP and PCP do not achieve conditional coverage and CHR and CQR performance is unstable. $\text{CP}^2\text{-PCP}$ on the other hand maintains valid conditional coverage on all clusters and even on outliers (cluster label -1). Not that these are all outliers combined and they may not lie in the same region of the input space.

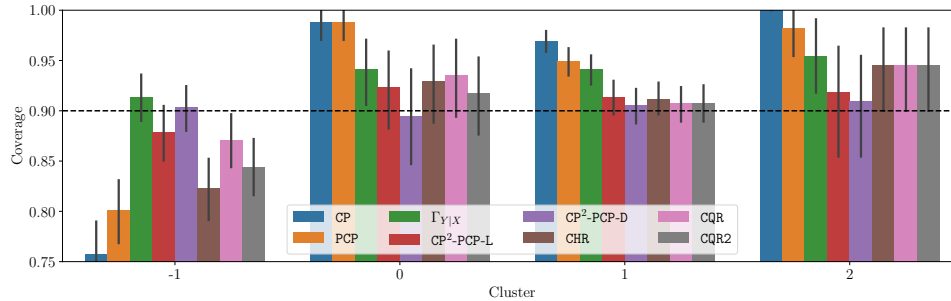


Figure 7: Conditional coverage for different clusters, fb1 dataset. We have used HDBSCAN algorithm with minimum cluster size of 100, `min_samples` hyper-parameter of 20 and l_2 metric. Cluster label -1 corresponds to the outliers. Sample size for sampling-based methods was set to 50. Nominal coverage equals $(1 - \alpha) = 0.9$ and is shown in dashed blacks.

5 Conclusion

We address the challenge of conditional coverage in conformal predictions, and overcome previous negative results by assuming the knowledge of a good estimator of $P_{Y|X}$. We develop a general framework for constructing prediction sets, which encompasses many existing conformal methods and refine their confidence sets using a probabilistic estimator of $Y | X$. Our key contributions include theoretical studies of the conditional validity, holding significant implications for the development of future methods.

Acknowledgments and Disclosure of Funding

Part of this work has been carried out under the auspice of the Lagrange Mathematics and Computing Research Center. E.M. is Funded by the European Union (ERC, Ocean, 101071601). Views and opinions expressed are however those of the author(s) only and do not necessarily reflect those of the European Union or the European Research Council Executive Agency. Neither the European Union nor the granting authority can be held responsible for them.

References

- [1] A. M. Alaa, Z. Hussain, and D. Sontag. Conformalized unconditional quantile regression. In *International Conference on Artificial Intelligence and Statistics*, pages 10690–10702. PMLR, 2023.
- [2] A. Beyerlein. Quantile regression—opportunities and challenges from a user’s perspective. *American journal of epidemiology*, 180(3):330–331, 2014.
- [3] M. Bian and R. F. Barber. Training-conditional coverage for distribution-free predictive inference. *Electronic Journal of Statistics*, 17(2):2044–2066, 2023.
- [4] C. M. Bishop. Mixture density networks. 1994.
- [5] S. Boucheron, G. Lugosi, and O. Bousquet. Concentration inequalities. In *Summer school on machine learning*, pages 208–240. Springer, 2003.
- [6] T. T. Cai, M. Low, and Z. Ma. Adaptive confidence bands for nonparametric regression functions. *Journal of the American Statistical Association*, 109(507):1054–1070, 2014.
- [7] R. J. G. B. Campello, D. Moulavi, and J. Sander. Density-based clustering based on hierarchical density estimates. In *Pacific-Asia Conference on Knowledge Discovery and Data Mining*, 2013.
- [8] M. Cauchois, S. Gupta, and J. C. Duchi. Knowing what you know: valid and validated confidence sets in multiclass and multilabel prediction. *J. Mach. Learn. Res.*, 22:81:1–81:42, 2020.

- [9] V. Chernozhukov, K. Wüthrich, and Y. Zhu. Distributional conformal prediction. *Proceedings of the National Academy of Sciences*, 118(48):e2107794118, 2021.
- [10] D. Cho, C. Yoo, J. Im, and D.-H. Cha. Comparative assessment of various machine learning-based bias correction methods for numerical weather prediction model forecasts of extreme air temperatures in urban areas. *Earth and Space Science*, 7(4):e2019EA000740, 2020.
- [11] N. Dewolf, B. De Baets, and W. Waegeman. Heteroskedastic conformal regression. *arXiv preprint arXiv:2309.08313*, 2023.
- [12] N. Diamant, E. Hajiramezani, T. Biancalani, and G. Scalia. Conformalized deep splines for optimal and efficient prediction sets. In *International Conference on Artificial Intelligence and Statistics*, pages 1657–1665. PMLR, 2024.
- [13] R. Foygel Barber, E. J. Candès, A. Ramdas, and R. J. Tibshirani. The limits of distribution-free conditional predictive inference. *Information and Inference: A Journal of the IMA*, 10(2):455–482, 2021.
- [14] A. Gendler, T.-W. Weng, L. Daniel, and Y. Romano. Adversarially robust conformal prediction. In *International Conference on Learning Representations*, 2021.
- [15] L. Guan. Conformal prediction with localization. *arXiv preprint arXiv:1908.08558*, 2019.
- [16] L. Guan. Localized conformal prediction: A generalized inference framework for conformal prediction. *Biometrika*, 110(1):33–50, 2023.
- [17] E. K. Guha, S. Natarajan, T. Möllenhoff, M. E. Khan, and E. Ndiaye. Conformal prediction via regression-as-classification. In *The Twelfth International Conference on Learning Representations*, 2024.
- [18] C. Gupta, A. K. Kuchibhotla, and A. Ramdas. Nested conformal prediction and quantile out-of-bag ensemble methods. *Pattern Recognition*, 127:108496, 2022.
- [19] X. Han, Z. Tang, J. Ghosh, and Q. Liu. Split localized conformal prediction. *arXiv preprint arXiv:2206.13092*, 2022.
- [20] R. Izbicki, G. Shimizu, and R. Stern. Flexible distribution-free conditional predictive bands using density estimators. In *International Conference on Artificial Intelligence and Statistics*, pages 3068–3077. PMLR, 2020.
- [21] R. Izbicki, G. Shimizu, and R. B. Stern. Cd-split and hpd-split: Efficient conformal regions in high dimensions. *The Journal of Machine Learning Research*, 23(1):3772–3803, 2022.
- [22] D. Kivaranovic, K. D. Johnson, and H. Leeb. Adaptive, distribution-free prediction intervals for deep networks. In *International Conference on Artificial Intelligence and Statistics*, pages 4346–4356. PMLR, 2020.
- [23] R. Koenker and K. F. Hallock. Quantile regression. *Journal of economic perspectives*, 15(4):143–156, 2001.
- [24] J. Lei, M. G’Sell, A. Rinaldo, R. J. Tibshirani, and L. Wasserman. Distribution-free predictive inference for regression. *Journal of the American Statistical Association*, 113(523):1094–1111, 2018.
- [25] J. Lei and L. Wasserman. Distribution-free prediction bands for non-parametric regression. *Journal of the Royal Statistical Society Series B: Statistical Methodology*, 76(1):71–96, 2014.
- [26] L. McInnes and J. Healy. Accelerated hierarchical density based clustering. *2017 IEEE International Conference on Data Mining Workshops (ICDMW)*, pages 33–42, 2017.
- [27] P. Melki, L. Bombrun, B. Diallo, J. Dias, and J.-P. Da Costa. Group-conditional conformal prediction via quantile regression calibration for crop and weed classification. In *Proceedings of the IEEE/CVF International Conference on Computer Vision*, pages 614–623, 2023.
- [28] V. Plassier, N. Kotelevskii, A. Rubashevskii, F. Noskov, M. Velikanov, A. Fishkov, S. Horvath, M. Takac, E. Moulines, and M. Panov. Efficient conformal prediction under data heterogeneity. In *International Conference on Artificial Intelligence and Statistics*, pages 4879–4887. PMLR, 2024.
- [29] Y. Romano, R. F. Barber, C. Sabatti, and E. Candès. With malice toward none: Assessing uncertainty via equalized coverage. *Harvard Data Science Review*, 2(2):4, 2020.

- [30] Y. Romano, E. Patterson, and E. Candes. Conformalized quantile regression. *Advances in neural information processing systems*, 32, 2019.
- [31] Y. Romano, M. Sesia, and E. Candes. Classification with valid and adaptive coverage. *Advances in Neural Information Processing Systems*, 33:3581–3591, 2020.
- [32] R. Rossellini, R. F. Barber, and R. Willett. Integrating uncertainty awareness into conformalized quantile regression. In *International Conference on Artificial Intelligence and Statistics*, pages 1540–1548. PMLR, 2024.
- [33] J. Rothfuss, F. Ferreira, S. Walther, and M. Ulrich. Conditional density estimation with neural networks: Best practices and benchmarks. *arXiv:1903.00954*, 2019.
- [34] M. Sesia and E. J. Candès. A comparison of some conformal quantile regression methods. *Stat*, 9(1):e261, 2020.
- [35] M. Sesia and Y. Romano. Conformal prediction using conditional histograms. *Advances in Neural Information Processing Systems*, 34:6304–6315, 2021.
- [36] G. Shafer and V. Vovk. A tutorial on conformal prediction. *Journal of Machine Learning Research*, 9(3), 2008.
- [37] A. W. Van der Vaart. *Asymptotic statistics*, volume 3. Cambridge university press, 2000.
- [38] V. Vovk. Conditional validity of inductive conformal predictors. In *Asian conference on machine learning*, pages 475–490. PMLR, 2012.
- [39] V. Vovk, A. Gammerman, and C. Saunders. Machine-learning applications of algorithmic randomness. In *Proceedings of the Sixteenth International Conference on Machine Learning*, pages 444–453, 1999.
- [40] V. Vovk, A. Gammerman, and G. Shafer. *Algorithmic learning in a random world*, volume 29. Springer, 2005.
- [41] Z. Wang, R. Gao, M. Yin, M. Zhou, and D. Blei. Probabilistic conformal prediction using conditional random samples. In *International Conference on Artificial Intelligence and Statistics*, pages 8814–8836. PMLR, 2023.

A Additional results and calculations

In this section, we analyze the theoretical results of Section 3. First, let’s recall the definition of the quantile function for any distribution μ living in \mathbb{R} . For any $\alpha \in (0, 1)$, the quantile $Q_{1-\alpha}(\mu)$ is defined by

$$Q_{1-\alpha}(\mu) = \inf \{t \in \mathbb{R} : \mu((-\infty, t]) \geq 1 - \alpha\}.$$

Given a measure $\Pi_{Y|X=x}$ defined on $\sigma(\mathcal{Y})$, we consider for all $x \in \mathbb{R}^d$, $z \in \mathcal{Z}$, the parameters $\tau_{x,z}$ and $\lambda_{x,y,z}$ given by

$$\begin{aligned} \tau_{x,z} &= \inf \{ \tau \in \mathbb{R} : \Pi_{Y|X=x}(\mathcal{R}_z(x; f_\tau(\varphi))) \geq 1 - \alpha \}, \\ \lambda_{x,y,z} &= \inf \{ \lambda \in \mathbb{R} : y \in \mathcal{R}_z(x; \lambda) \}, \end{aligned} \quad (7)$$

where φ is chosen as in **H2**, and by convention we set $\inf \emptyset = \infty$. We denote by δ_v the Dirac measure at $v \in \mathbb{R}$, and write $\bar{\tau}_k = \tau_{X_k, Z_k}$ and $\bar{\lambda}_k = \lambda_{X_k, Y_k, Z_k}$. In this Appendix, we study the coverage of the prediction set given $\forall (x, z) \in \mathbb{R} \times \mathcal{Z}$ by

$$\mathcal{C}_\alpha(x) = \mathcal{R}_z(x; f_{\tau_{x,z}}(Q_{1-\alpha}(\mu))),$$

where the distribution μ is defined as

$$\mu = \frac{1}{n+1} \sum_{k=1}^n \delta_{f_{\bar{\tau}_k}^{-1}(\bar{\lambda}_k)} + \frac{1}{n+1} \delta_\infty.$$

The key idea behind the choice of $\bar{\tau}_k$ is to ensure that the conditional coverage of the prediction set $\mathcal{C}_\alpha(X_k)$ is approximately $1 - \alpha$ when the empirical distribution $\Pi_{Y|X=X_k}$ is close to $\mathbb{P}_{Y|X=X_k}$. In other words, $\bar{\tau}_k$ is chosen such that the probability of the observed value Y_k given X_k falling inside the prediction set $\mathcal{C}_\alpha(X_k)$ is close to $1 - \alpha$. On the other hand, the parameter λ_k is used to ensure that the prediction set $\mathcal{R}_{Z_k}(X_k; \bar{\lambda}_k)$ contains the observed value Y_k . Moreover, note that $\bar{\tau}_k$ only depends on the input data (X_k, Z_k) , while $\bar{\lambda}_k$ depends on (X_k, Y_k, Z_k) . Thus, the i.i.d. property of $\{(X_k, Y_k, Z_k) : k \in [n+1]\}$ ensures that the $\{(\bar{\tau}_k, \bar{\lambda}_k)\}_{k=1}^{n+1}$ are also i.i.d.

A.1 Proof of Theorems 3.1 and 3.2

Lemma A.1. Assume **H1** hold. For any $(x, y, z) \in \mathbb{R}^d \times \mathcal{Y} \times \mathcal{Z}$, $\lambda_{x,y,z}$ exists in \mathbb{R} , and we have $y \in \mathcal{R}_z(x; \lambda_{x,y,z})$.

Proof. Let $(x, y, z) \in \mathbb{R}^d \times \mathcal{Y} \times \mathcal{Z}$ be fixed. Since $\bigcap_{t \in \mathbb{R}} \mathcal{R}_z(x; t) = \emptyset$ and $\bigcup_{t \in \mathbb{R}} \mathcal{R}_z(x; t) = \mathcal{Y}$, we deduce the existence of t_0 and t_1 such that $y \notin \mathcal{R}_z(x; t_0)$ and $y \in \mathcal{R}_z(x; t_1)$. Therefore, $\{t \in \mathbb{R}: y \in \mathcal{R}_z(x; t)\}$ is non-empty and lower-bounded by t_0 . Thus, the infimum $\lambda_{x,y,z}$ exists. Now, let's prove that $y \in \mathcal{R}_z(x; \lambda_{x,y,z})$. Since $\lambda_{x,y,z} = \inf\{t \in \mathbb{R}: y \in \mathcal{R}_z(x; t)\}$, we deduce the existence of a decreasing sequence $\{\lambda_n\}_{n \in \mathbb{N}}$ such that $y \in \mathcal{R}_z(x; \lambda_n)$ and $\lim_{n \rightarrow \infty} \lambda_n = \lambda_{x,y,z}$. By definition of $\{\lambda_n\}_{n \in \mathbb{N}}$, we have $y \in \bigcap_{n \in \mathbb{N}} \mathcal{R}_z(x; \lambda_n)$. However, using **H1**, remark that

$$\begin{aligned} \bigcap_{n \in \mathbb{N}} \mathcal{R}_z(x; \lambda_n) &= \bigcap_{n \in \mathbb{N}} \bigcap_{t > \lambda_n} \mathcal{R}_z(x; t) \\ &= \bigcap_{t > \lim_{n \rightarrow \infty} \lambda_n} \mathcal{R}_z(x; t) \\ &= \bigcap_{t > \lambda_{x,y,z}} \mathcal{R}_z(x; t) = \mathcal{R}_z(x; \lambda_{x,y,z}). \end{aligned}$$

Since $y \in \bigcap_{n \in \mathbb{N}} \mathcal{R}_z(x; \lambda_n)$, it implies that $y \in \mathcal{R}_z(x; \lambda_{x,y,z})$. \square

We will now present the proof for Theorem 3.1, which establishes the marginal validity of our proposed method.

Theorem A.2. Assume **H1-H2** hold, if $\{f_{\bar{\tau}_k}^{-1}(\bar{\lambda}_k)\}_{k=1}^{n+1}$ are almost surely distinct, then it follows

$$1 - \alpha \leq \mathbb{P}(Y_{n+1} \in \mathcal{C}_\alpha(X_{n+1})) < 1 - \alpha + \frac{1}{n+1}. \quad (8)$$

Proof. By definition, we have

$$\begin{aligned} \mathbb{P}(Y_{n+1} \in \mathcal{C}_\alpha(X_{n+1})) &= \mathbb{P}(Y_{n+1} \in \mathcal{R}_{Z_{n+1}}(X_{n+1}, f_{\bar{\tau}_{n+1}}(Q_{1-\alpha}(\mu)))) \\ &= \mathbb{P}(\lambda_{n+1} \leq f_{\bar{\tau}_{n+1}}(Q_{1-\alpha}(\mu))). \end{aligned}$$

Since $\lambda \mapsto f_{\bar{\tau}_{n+1}}(\lambda)$ is increasing by **H2**, we deduce that

$$\mathbb{P}(\lambda_{n+1} \leq f_{\bar{\tau}_{n+1}}(Q_{1-\alpha}(\mu))) = \mathbb{P}(f_{\bar{\tau}_{n+1}}^{-1}(\lambda_{n+1}) \leq Q_{1-\alpha}(\mu)).$$

Denote by $V_k = f_{\bar{\tau}_k}^{-1}(\bar{\lambda}_k)$, the exchangeability of the data $\{(X_k, Y_k, Z_k): k \in [n+1]\}$ implies that

$$\begin{aligned} \mathbb{P}\left(V_{n+1} \leq Q_{1-\alpha}\left(\sum_{k=1}^n \frac{\delta_{V_k}}{n+1} + \frac{\delta_\infty}{n+1}\right)\right) &= \mathbb{P}\left(V_{n+1} \leq Q_{1-\alpha}\left(\sum_{k=1}^{n+1} \frac{\delta_{V_k}}{n+1}\right)\right) \\ &= \frac{1}{n+1} \sum_{k=1}^{n+1} \mathbb{E}\left[\mathbb{1}_{V_k} \leq Q_{1-\alpha}\left(\frac{1}{n+1} \sum_{k=1}^{n+1} \delta_{V_k}\right)\right] \\ &= \mathbb{E}\left[\mathbb{E}\left[\mathbb{1}_{V_I} \leq Q_{1-\alpha}\left(\frac{1}{n+1} \sum_{k=1}^{n+1} \delta_{V_k}\right) \mid V_1, \dots, V_{n+1}\right]\right], \end{aligned}$$

where $I \sim \text{Unif}(1, \dots, n+1)$. Therefore, the definition of the quantile function implies the lower bound in (8). Moreover, if there are no ties between the $\{V_k\}_{k=1}^{n+1}$, then

$$\mathbb{P}\left(f_{\bar{\tau}_{n+1}}^{-1}(\lambda_{n+1}) \leq Q_{1-\alpha}(\mu)\right) < 1 - \alpha + \frac{1}{n+1}. \quad \square$$

The following lemma provides conditions under which $\mathbb{P}_{Y|X=x}(\mathcal{R}_z(x; f_{\tau_{x,z}}(\varphi))) \geq 1 - \alpha$.

Lemma A.3. Assume **H1-H2** hold, and let $\alpha \in (0, 1)$, $x \in \mathbb{R}^d$, $z \in \mathcal{Z}$. If $\mathbb{P}_{Y|X=x}$ is a probability measure, then $\tau_{x,z}$ is defined in \mathbb{R} and $\mathbb{P}_{Y|X=x}(\mathcal{R}_z(x; f_{\tau_{x,z}}(\varphi))) \geq 1 - \alpha$.

Proof. Let $x \in \mathbb{R}^d$ be such that $\Pi_{Y|X=x}$ is a probability measure, and fix $z \in \mathcal{Z}$. Since $\tau \mapsto f_\tau(\varphi)$ is increasing and bijective by **H2**, we have

$$\begin{aligned} \lim_{\tau \rightarrow +\infty} \Pi_{Y|X=x}(\mathcal{R}_z(x; f_\tau(\varphi))) &= \Pi_{Y|X=x}(\cup_{\tau \in \mathbb{R}} \mathcal{R}_z(x; f_\tau(\varphi))) \\ &= \Pi_{Y|X=x}(\cup_{t \in \mathbb{R}} \mathcal{R}_z(x; t)) = 1. \end{aligned}$$

The previous equality shows the existence of $\tau \in \mathbb{R}$ such that $\Pi_{Y|X=x}(\mathcal{R}_z(x; f_\tau(\varphi))) \geq 1 - \alpha$. Therefore $\{\tau \in \mathbb{R} : \Pi_{Y|X=x}(\mathcal{R}_z(x; f_\tau(\varphi))) \geq 1 - \alpha\}$ is non-empty. This proves the existence of $\tau_{x,z} = \inf\{\tau \in \mathbb{R} : \Pi_{Y|X=x}(\mathcal{R}_z(x; f_\tau(\varphi))) \geq 1 - \alpha\}$ in $\mathbb{R} \cup \{-\infty\}$. However, $\tau_{x,z} > -\infty$, otherwise we would have

$$1 - \alpha \leq \lim_{\tau \rightarrow -\infty} \Pi_{Y|X=x}(\mathcal{R}_z(x; f_\tau(\varphi))) = \Pi_{Y|X=x}(\cap_{t \in \mathbb{R}} \mathcal{R}_z(x; t)) = \Pi_{Y|X=x}(\emptyset) = 0.$$

Therefore, we deduce that $\tau_{x,z} \in \mathbb{R}$. Lastly, remark that

$$\begin{aligned} \Pi_{Y|X=x}(\mathcal{R}_z(x; f_{\tau_{x,z}}(\varphi))) &= \Pi_{Y|X=x}(\cap_{\tau > \tau_{x,z}} \mathcal{R}_z(x; f_\tau(\varphi))) \\ &= \inf_{\tau > \tau_{x,z}} \Pi_{Y|X=x}(\mathcal{R}_z(x; f_\tau(\varphi))) \geq 1 - \alpha. \end{aligned}$$

□

Now, we prove Theorem 3.2. This result guarantees that the conditional confidence intervals constructed by our method approximately satisfy the desired coverage of $1 - \alpha$.

Theorem A.4. Assume **H1-H2** hold, let $x \in \mathbb{R}^d$ be such that $\Pi_{Y|X=x}$ is a probability measure. For any $z \in \mathcal{Z}$, it follows that

$$\begin{aligned} \mathbb{P}(Y_{n+1} \in \mathcal{C}_\alpha(X_{n+1}) \mid X_{n+1} = x, Z_{n+1} = z) &\geq 1 - \alpha - d_{\text{TV}}(\mathbb{P}_{Y|X=x}; \Pi_{Y|X=x}) \\ &\quad - \mathbb{P}\left(Q_{1-\alpha}(\mu) < f_{\tau_{x,z}}^{-1}(\lambda_{x,Y_{n+1},z}) \leq \varphi \mid X_{n+1} = x, Z_{n+1} = z\right). \end{aligned}$$

Proof. First, recall that $\mathcal{C}_\alpha(x)$ is given in (4), and $\lambda_{x,Y_{n+1},z}$ is defined in (7). Applying Lemma A.1, we know that $\lambda_{x,Y_{n+1},z}$ is defined in \mathbb{R} , and also that $Y_{n+1} \in \mathcal{R}_z(x; \lambda_{x,Y_{n+1},z})$. Hence, it holds

$$\begin{aligned} &\mathbb{P}(Y_{n+1} \in \mathcal{C}_\alpha(X_{n+1}) \mid X_{n+1} = x, Z_{n+1} = z) \\ &= \mathbb{P}(Y_{n+1} \in \mathcal{R}_z(x; f_{\tau_{x,z}}(Q_{1-\alpha}(\mu))) \mid X_{n+1} = x, Z_{n+1} = z) \\ &= \mathbb{P}(\lambda_{x,Y_{n+1},z} \leq f_{\tau_{x,z}}(Q_{1-\alpha}(\mu)) \mid X_{n+1} = x, Z_{n+1} = z). \end{aligned}$$

Let's introduce the term $\mathbb{P}(\lambda_{x,Y_{n+1},z} \leq f_{\tau_{x,z}}(\varphi) \mid X_{n+1} = x, Z_{n+1} = z)$ as follows:

$$\begin{aligned} &\mathbb{P}(\lambda_{x,Y_{n+1},z} \leq f_{\tau_{x,z}}(Q_{1-\alpha}(\mu)) \mid X_{n+1} = x, Z_{n+1} = z) \\ &= \mathbb{P}(\lambda_{x,Y_{n+1},z} \leq f_{\tau_{x,z}}(Q_{1-\alpha}(\mu)) \mid X_{n+1} = x, Z_{n+1} = z) \\ &\quad \pm \mathbb{P}(\lambda_{x,Y_{n+1},z} \leq f_{\tau_{x,z}}(\varphi) \mid X_{n+1} = x, Z_{n+1} = z). \quad (9) \end{aligned}$$

Now, we will control the difference between the two terms of the previous equation. Let A and B be defined as

$$\begin{aligned} A &= \mathbb{P}\left(f_{\tau_{x,z}}^{-1}(\lambda_{x,Y_{n+1},z}) \leq Q_{1-\alpha}(\mu) < \varphi \mid X_{n+1} = x, Z_{n+1} = z\right), \\ B &= \mathbb{P}\left(f_{\tau_{x,z}}^{-1}(\lambda_{x,Y_{n+1},z}) \leq \varphi \leq Q_{1-\alpha}(\mu) \mid X_{n+1} = x, Z_{n+1} = z\right). \end{aligned}$$

We have

$$\begin{aligned} &\mathbb{P}(\lambda_{x,Y_{n+1},z} \leq f_{\tau_{x,z}}(Q_{1-\alpha}(\mu)) \mid X_{n+1} = x, Z_{n+1} = z) \\ &= A + B + \mathbb{P}\left(\varphi < f_{\tau_{x,z}}^{-1}(\lambda_{x,Y_{n+1},z}) \leq Q_{1-\alpha}(\mu) \mid X_{n+1} = x, Z_{n+1} = z\right), \end{aligned}$$

and also

$$\begin{aligned} &\mathbb{P}(\lambda_{x,Y_{n+1},z} \leq f_{\tau_{x,z}}(\varphi) \mid X_{n+1} = x, Z_{n+1} = z) \\ &= A + B + \mathbb{P}\left(Q_{1-\alpha}(\mu) < f_{\tau_{x,z}}^{-1}(\lambda_{x,Y_{n+1},z}) \leq \varphi \mid X_{n+1} = x, Z_{n+1} = z\right). \end{aligned}$$

Therefore, the difference between the terms introduced in (9) can be rewritten as

$$\begin{aligned}
& \mathbb{P}(\lambda_{x, Y_{n+1}, z} \leq f_{\tau_{x,z}}(Q_{1-\alpha}(\mu)) \mid X_{n+1} = x, Z_{n+1} = z) \\
& \quad - \mathbb{P}(\lambda_{x, Y_{n+1}, z} \leq f_{\tau_{x,z}}(\varphi) \mid X_{n+1} = x, Z_{n+1} = z) \\
& = \mathbb{P}\left(\varphi < f_{\tau_{x,z}}^{-1}(\lambda_{x, Y_{n+1}, z}) \leq Q_{1-\alpha}(\mu) \mid X_{n+1} = x, Z_{n+1} = z\right) \\
& \quad - \mathbb{P}\left(Q_{1-\alpha}(\mu) < f_{\tau_{x,z}}^{-1}(\lambda_{x, Y_{n+1}, z}) \leq \varphi \mid X_{n+1} = x, Z_{n+1} = z\right). \quad (10)
\end{aligned}$$

By definition of the total variation distance, we have

$$\begin{aligned}
& \mathbb{P}(\lambda_{x, Y_{n+1}, z} \leq f_{\tau_{x,z}}(\varphi) \mid X_{n+1} = x, Z_{n+1} = z) \\
& \geq \mathbb{P}(\lambda_{x, \hat{Y}_{n+1}, z} \leq f_{\tau_{x,z}}(\varphi) \mid X_{n+1} = x, Z_{n+1} = z) - \text{d}_{\text{TV}}(\mathbb{P}_{Y|X=x}; \Pi_{Y|X=x}).
\end{aligned}$$

Moreover, Lemma A.3 implies that

$$\begin{aligned}
& \mathbb{P}(\lambda_{x, \hat{Y}_{n+1}, z} \leq f_{\tau_{x,z}}(\varphi) \mid X_{n+1} = x, Z_{n+1} = z) \\
& = \mathbb{P}(\hat{Y}_{n+1} \in \{y \in \mathcal{Y} : \lambda_{x,y,z} \leq f_{\tau_{x,z}}(\varphi)\} \mid X_{n+1} = x, Z_{n+1} = z) \\
& = \mathbb{P}(\hat{Y}_{n+1} \in \mathcal{R}_z(x; f_{\tau_{x,z}}(\varphi)) \mid X_{n+1} = x, Z_{n+1} = z) \\
& = \Pi_{Y|X=x}(\mathcal{R}_z(x; f_{\tau_{x,z}}(\varphi))) \geq 1 - \alpha.
\end{aligned}$$

Therefore, we deduce that

$$\mathbb{P}(\lambda_{x, Y_{n+1}, z} \leq f_{\tau_{x,z}}(\varphi) \mid X_{n+1} = x, Z_{n+1} = z) \geq 1 - \alpha - \text{d}_{\text{TV}}(\mathbb{P}_{Y|X=x}; \Pi_{Y|X=x}).$$

Finally, combining the previous result with (9) and (10) shows that

$$\begin{aligned}
& \mathbb{P}(\lambda_{x, Y_{n+1}, z} \leq f_{\tau_{x,z}}(Q_{1-\alpha}(\mu)) \mid X_{n+1} = x, Z_{n+1} = z) \geq 1 - \alpha - \text{d}_{\text{TV}}(\mathbb{P}_{Y|X=x}; \Pi_{Y|X=x}) \\
& \quad + \mathbb{P}\left(\varphi < f_{\tau_{x,z}}^{-1}(\lambda_{x, Y_{n+1}, z}) \leq Q_{1-\alpha}(\mu) \mid X_{n+1} = x, Z_{n+1} = z\right) \\
& \quad - \mathbb{P}\left(Q_{1-\alpha}(\mu) < f_{\tau_{x,z}}^{-1}(\lambda_{x, Y_{n+1}, z}) \leq \varphi \mid X_{n+1} = x, Z_{n+1} = z\right).
\end{aligned}$$

□

A.2 Proof of Corollary 3.3

The objective of this section is to study the conditional guarantee obtained in Theorem A.4. Under some assumptions, we have demonstrated that the conditional coverage is controlled as follows:

$$\begin{aligned}
& \mathbb{P}(Y_{n+1} \in \mathcal{C}_\alpha(X_{n+1}) \mid X_{n+1} = x, Z_{n+1} = z) \geq 1 - \alpha - \text{d}_{\text{TV}}(\mathbb{P}_{Y|X=x}; \Pi_{Y|X=x}) - p_{n+1}^{(x,z)}, \\
& p_{n+1}^{(x,z)} = \mathbb{P}\left(Q_{1-\alpha}(\mu) < f_{\tau_{x,z}}^{-1}(\lambda_{x, Y_{n+1}, z}) \leq \varphi \mid X_{n+1} = x, Z_{n+1} = z\right),
\end{aligned}$$

where $\mu = \frac{1}{n+1} \sum_{k=1}^n \delta_{f_{\tau_{X_k}}^{-1}(\bar{\lambda}_k)} + \frac{1}{n+1} \delta_\infty$. While $\mathbb{E}[p_{n+1}^{(X_{n+1}, Z_{n+1})}] \leq \alpha$, studying $p_{n+1}^{(x,z)}$ is challenging. However, we control this term in Corollary A.5. Remark, the quantile $Q_{1-\alpha}(\mu)$ is an order statistic with a known distribution that rapidly converges to the true quantile q_0 , which is defined for any $\epsilon \in [0, 1 - \alpha]$ by

$$q_\epsilon = \inf\{t \in \mathbb{R} : \mathbb{P}(f_{\tau_{X,Z}}^{-1}(\lambda_{X,Y,Z}) \leq t) \geq 1 - \alpha - \epsilon\}. \quad (11)$$

Moreover, we define the cumulative density functions $F : t \mapsto \mathbb{P}(f_{\tau_{X,Z}}^{-1}(\lambda_{X,Y,Z}) \leq t)$ and $\hat{F} : t \mapsto \mathbb{P}(f_{\tau_{X,Z}}^{-1}(\lambda_{X,\hat{Y},Z}) \leq t)$, where $(X, Y, Z) \sim \mathbb{P}_X \otimes \mathbb{P}_{Y|X} \otimes \Pi_{Z|X}$ and $(X, \hat{Y}, Z) \sim \mathbb{P}_X \otimes \Pi_{Y|X} \otimes \Pi_{Z|X}$.

Corollary A.5. Assume **H1-H2** hold, and let $x \in \mathbb{R}^d$ be such that $\Pi_{Y|X=x}$ is a probability measure. For any $\epsilon \in [0, 1 - \alpha]$, if $p_\epsilon = \mathbb{P}(f_{\tau_{X,Z}}^{-1}(\lambda_{X,Y,Z}) < q_\epsilon) \leq 1 - \alpha$, then it follows that

$$p_{n+1}^{(x,z)} \leq \mathbb{P}\left(F^{-1}(1 - \alpha - \epsilon) < f_{\tau_{x,y}}^{-1}(\lambda_{x,Y_{n+1},z}) \leq \hat{F}^{-1}(1 - \alpha) \mid X_{n+1} = x, Z_{n+1} = z\right) \\ + \exp\left(-np_\epsilon(1 - p_\epsilon)h\left(\frac{1 - \alpha - p_\epsilon}{p_\epsilon(1 - p_\epsilon)}\right)\right),$$

where $h : u \mapsto (1 + u) \log(1 + u) - u$.

Proof. Let $\epsilon \in [0, 1 - \alpha]$, $x \in \mathbb{R}^d$, and consider

$$A = \{Q_{1-\alpha}(\mu) < q_\epsilon\}, \\ B_{x,z} = \{y \in \mathcal{Y} : f_{\tau_{x,z}}(q_\epsilon) < \lambda_{x,y,z} \leq f_{\tau_{x,z}}(\varphi)\}.$$

We have

$$\mathbb{P}(f_{\tau_{x,z}}(Q_{1-\alpha}(\mu)) < \lambda_{x,Y_{n+1},z} \leq f_{\tau_{x,z}}(\varphi) \mid X_{n+1} = x, Z_{n+1} = z) \\ \leq \mathbb{P}(A \mid X_{n+1} = x, Z_{n+1} = z) + \mathbb{P}(Y_{n+1} \in B_{x,z} \mid X_{n+1} = x, Z_{n+1} = z).$$

Now, let's upper bound the first term of the right-hand side equation. First, remark that

$$\{Q_{1-\alpha}(\mu) < q_\epsilon\} \Leftrightarrow \left\{ \frac{1}{n+1} \sum_{k=1}^n \mathbb{1}_{f_{\tau_k}^{-1}(\bar{\lambda}_k) < q_\epsilon} \geq 1 - \alpha \right\}.$$

Thus, we deduce that

$$\mathbb{P}(A \mid X_{n+1} = x, Z_{n+1} = z) \leq \mathbb{P}\left(\sum_{k=1}^n \mathbb{1}_{f_{\tau_k}^{-1}(\bar{\lambda}_k) < q_\epsilon} \geq (n+1)(1 - \alpha)\right).$$

Recall that $p_\epsilon = \mathbb{P}(f_{\tau_{X,Z}}^{-1}(\lambda_{X,Y,Z}) < q_\epsilon)$, and also that we assume $p_\epsilon \leq 1 - \alpha$. Therefore, the Bennett's inequality [5, Theorem 2] implies that

$$\mathbb{P}(A \mid X_{n+1} = x, Z_{n+1} = z) \leq \exp\left(-np_\epsilon(1 - p_\epsilon)h\left(\frac{(n+1)(1 - \alpha) - np_\epsilon}{np_\epsilon(1 - p_\epsilon)}\right)\right), \quad (12)$$

where $h : u \mapsto (1 + u) \log(1 + u) - u$. Moreover, define

$$u_\epsilon = \frac{1 - \alpha - p_\epsilon}{p_\epsilon(1 - p_\epsilon)}, \quad \tilde{u}_\epsilon = \frac{(n+1)(1 - \alpha) - np_\epsilon}{np_\epsilon(1 - p_\epsilon)}.$$

We have $\tilde{u}_\epsilon \leq u_\epsilon$, from the increasing property of h it follows that

$$\mathbb{P}(A \mid X_{n+1} = x, Z_{n+1} = z) \leq \exp(-np_\epsilon(1 - p_\epsilon)h(u_\epsilon)).$$

Furthermore, the definition of the cumulative distribution function:

$$\mathbb{P}(Y_{n+1} \in B_{x,z} \mid X_{n+1} = x, Z_{n+1} = z) \\ = \mathbb{P}(f_{\tau_{x,z}}(q_\epsilon) < \lambda_{x,Y_{n+1},z} \leq f_{\tau_{x,z}}(\varphi) \mid X_{n+1} = x, Z_{n+1} = z).$$

By definition of q_ϵ provided in (11), we have $q_\epsilon = F^{-1}(1 - \alpha - \epsilon)$. Moreover, for any $t \in (-\infty, \varphi)$, we have

$$\hat{F}(t) = \mathbb{P}\left(f_{\tau_{X,Z}}^{-1}(\lambda_{X,\hat{Y},Z}) \leq t\right) \\ = \int \mathbb{P}\left(f_{\tau_{X,Z}}^{-1}(\lambda_{X,\hat{Y},Z}) \leq t \mid X = x, Z = z\right) \Pi_{Z|X=x}(dz) \mathbf{P}_X(dx) \\ = \int \mathbb{P}\left(\hat{Y} \in \mathcal{R}(x, f_{\tau_{x,z}}(t)) \mid X = x, Z = z\right) \Pi_{Z|X=x}(dz) \mathbf{P}_X(dx).$$

Using **H2**, the bijective property of $\tau \mapsto f_\tau(\varphi)$ implies the existence of $\nu \in \mathbb{R}$, such that $f_\nu(\varphi) = f_{\tau_{x,z}}(t)$. Note that, $\nu < \tau_{x,z}$ otherwise it would lead to $f_\nu(\varphi) \geq f_{\tau_{x,z}}(\varphi) > f_{\tau_{x,z}}(t)$. The definition of $\tau_{x,z}$ shows that

$$\mathbb{P}\left(\hat{Y} \in \mathcal{R}(x, f_\nu(\varphi)) \mid X = x, Z = z\right) < 1 - \alpha.$$

Therefore, we deduce that $\hat{F}^{-1}(1 - \alpha) \geq \varphi$, and we can conclude that

$$\begin{aligned} & \mathbb{P}(Y_{n+1} \in B_{x,z} \mid X_{n+1} = x, Z_{n+1} = z) \\ & \leq \mathbb{P}\left(F^{-1}(1 - \alpha - \epsilon) < f_{\tau_{x,y}}^{-1}(\lambda_{x,Y_{n+1},z}) \leq \hat{F}^{-1}(1 - \alpha) \mid X_{n+1} = x, Z_{n+1} = z\right). \end{aligned} \quad (13)$$

Finally, combining (12) and (13) concludes the proof. \square

Given $\alpha \in (0, 1)$, define the threshold

$$\epsilon_n = \sqrt{\frac{8\alpha(1 - \alpha) \log n}{n}}.$$

Lemma A.6. *If the distribution of $f_{\tau_{X,Z}}^{-1}(\lambda_{X,Y,Z})$ is continuous, then for all $\epsilon \in [0, 1 - \alpha)$, we have $p_\epsilon = \mathbb{P}(f_{\tau_{X,Z}}^{-1}(\lambda_{X,Y,Z}) < q_\epsilon) = 1 - \alpha - \epsilon$. Moreover, if $\epsilon_n \leq \frac{\alpha(1 - \alpha)}{8}$, then it follows*

$$\exp\left(-np_{\epsilon_n}(1 - p_{\epsilon_n})h\left(\frac{1 - \alpha - p_{\epsilon_n}}{p_{\epsilon_n}(1 - p_{\epsilon_n})}\right)\right) \leq \frac{1}{n},$$

where $h : u \mapsto (1 + u) \log(1 + u) - u$.

Proof. First, recall that q_ϵ is defined in (11). If the distribution of $f_{\tau_{X,Z}}^{-1}(\lambda_{X,Y,Z})$ is continuous, then we have

$$1 - \alpha - \epsilon \leq F(q_\epsilon) = \sup_{\delta > 0} F(q_\epsilon - \delta) \leq \mathbb{P}\left(f_{\tau_{X,Z}}^{-1}(\lambda_{X,Y,Z}) < q_\epsilon\right) = p_\epsilon \leq 1 - \alpha - \epsilon.$$

Therefore, we deduce that $p_\epsilon = 1 - \alpha - \epsilon$. Let's denote

$$\delta_n = (n + 1)(1 - \alpha) - np_{\epsilon_n}, \quad u_n = \frac{(n + 1)(1 - \alpha) - np_{\epsilon_n}}{np_{\epsilon_n}(1 - p_{\epsilon_n})}.$$

For any $u \geq 0$, remark that $\log(1 + u) \geq u - u^2/2$. Thus, we deduce

$$\begin{aligned} np_{\epsilon_n}(1 - p_{\epsilon_n})h(u_n) & \geq \delta_n \frac{(1 + u_n) \log(1 + u_n) - u_n}{u_n} \\ & \geq \delta_n \frac{u_n(1 - u_n)}{2}. \end{aligned} \quad (14)$$

Now, let's show that $u_n \leq 1/4$. We have

$$\begin{aligned} u_n & = \frac{(n + 1)(1 - \alpha) - np_{\epsilon_n}}{np_{\epsilon_n}(1 - p_{\epsilon_n})} \\ & = \frac{1 - \alpha}{np_{\epsilon_n}(1 - p_{\epsilon_n})} + \frac{1 - \alpha - p_{\epsilon_n}}{p_{\epsilon_n}(1 - p_{\epsilon_n})} \\ & = \frac{1 - \alpha}{n(\alpha + \epsilon_n)(1 - \alpha - \epsilon_n)} + \frac{\epsilon_n}{(\alpha + \epsilon_n)(1 - \alpha - \epsilon_n)}. \end{aligned}$$

Therefore, $u_n \leq 1/4$ if and only if

$$\frac{1 - \alpha}{n} + \epsilon_n \leq \frac{(\alpha + \epsilon_n)(1 - \alpha - \epsilon_n)}{4}.$$

The function $\epsilon \in [0, 1/2 - \alpha] \mapsto (\alpha + \epsilon)(1 - \alpha - \epsilon)$ is increasing. Since $\epsilon_n \leq \alpha(1 - \alpha)/8 \leq 1/2 - \alpha$, it is sufficient to prove that

$$\frac{1 - \alpha}{n} + \epsilon_n \leq \frac{\alpha(1 - \alpha)}{4}.$$

Since $\epsilon_n \leq \alpha(1 - \alpha)/8$, we just need to show that

$$\frac{1 - \alpha}{n} \leq \frac{\alpha(1 - \alpha)}{8}, \quad \text{i.e.,} \quad \frac{8\alpha(1 - \alpha)}{n} \leq \alpha^2(1 - \alpha). \quad (15)$$

Again, using the fact that $\epsilon_n \leq \alpha(1 - \alpha)/8$, we deduce that

$$\frac{8\alpha(1 - \alpha)}{n} = \frac{\epsilon_n^2}{\log n} \leq \frac{\alpha^2(1 - \alpha)^2}{8 \log n} = \alpha^2(1 - \alpha) \times \frac{(1 - \alpha)}{8 \log n}.$$

Since $\frac{(1 - \alpha)}{8 \log n} \leq 1$, we deduce that (15) holds. This concludes that $u_n \leq 1/4$. Moreover, for any $u \in [0, 0.25]$, we have

$$\delta_n \frac{u(1 - u)}{2} \geq \frac{u\delta_n}{4}.$$

Plugging the previous line in (14) implies that

$$\begin{aligned} \exp(-np_{\epsilon_n}(1 - p_{\epsilon_n})h(u_n)) &\leq \exp\left(-\frac{[(n + 1)(1 - \alpha) - np_{\epsilon_n}]^2}{4np_{\epsilon_n}(1 - p_{\epsilon_n})}\right) \\ &\leq \exp\left(-\frac{(1 - \alpha + n\epsilon_n)^2}{4n(\alpha + \epsilon_n)(1 - \alpha - \epsilon_n)}\right) \\ &\leq \exp\left(-\frac{n\epsilon_n^2}{4(\alpha + \epsilon_n)(1 - \alpha - \epsilon_n)}\right). \end{aligned} \quad (16)$$

Lastly, since $\epsilon_n \leq \alpha$, it follows that

$$\frac{n\epsilon_n^2}{4(\alpha + \epsilon_n)(1 - \alpha - \epsilon_n)} = \frac{2\alpha(1 - \alpha) \log n}{(\alpha + \epsilon_n)(1 - \alpha - \epsilon_n)} \geq \log n.$$

Combining the previous line with (16) completes the proof. \square

A.3 Proof of Corollary 3.4

In this last part of Appendix A, we prove a corollary of Theorem 3.1. Its result demonstrates the marginal validity of the prediction set defined as

$$\bar{\mathcal{C}}_\alpha(x) = \mathcal{R}_z\left(x; f_{\tau_{x,z}}\left(Q_{(1-\alpha)(1+n^{-1})}\left(\frac{1}{n} \sum_{k=1}^n \delta_{f_{\bar{\tau}_k}^{-1}(\bar{\lambda}_k)}\right)\right)\right). \quad (17)$$

The prediction set $\bar{\mathcal{C}}_\alpha(x)$ relies on the quantile of the distribution $\frac{1}{n} \sum_{k=1}^n \delta_{f_{\bar{\tau}_k}^{-1}(\bar{\lambda}_k)}$. However, the proof reveals that this prediction set is equivalent to $\mathcal{C}_\alpha(x)$.

Corollary A.7. *Under the same assumptions as in Theorem 3.1, for any $\alpha \in [1/(n + 1), 1]$, we have*

$$1 - \alpha \leq \mathbb{P}(Y_{n+1} \in \bar{\mathcal{C}}_\alpha(X_{n+1})) < 1 - \alpha + \frac{1}{n + 1},$$

where the upper bound only holds if $\{f_{\bar{\tau}_k}^{-1}(\bar{\lambda}_k)\}_{k=1}^{n+1}$ are almost surely distinct.

Proof. Let $\alpha \in \mathbb{R}$ such that $(n + 1)^{-1} \leq \alpha \leq 1$, and recall that

$$\mu = \frac{1}{n + 1} \sum_{k=1}^n \delta_{f_{\bar{\tau}_k}^{-1}(\bar{\lambda}_k)} + \frac{1}{n + 1} \delta_\infty.$$

Since $\alpha \geq (n + 1)^{-1}$, the quantile $Q_{1-\alpha}(\mu)$ is the k_α th order statistic of V_1, \dots, V_n , where

$$V_k = f_{\bar{\tau}_k}^{-1}(\bar{\lambda}_k), \quad \text{and} \quad k_\alpha = \lceil (1 - \alpha)(n + 1) \rceil.$$

However, $\forall \beta \in (\frac{k_\alpha - 1}{n}, \frac{k_\alpha}{n}]$, we have

$$Q_\beta\left(\frac{1}{n} \sum_{k=1}^n \delta_{V_k}\right) = V_{(k_\alpha)}.$$

Since $\mathcal{C}_\alpha(X_{n+1}) = \mathcal{R}_{Z_{n+1}}(X_{n+1}; f_{\bar{\tau}_{n+1}}(V_{(k_\alpha)}))$, Theorem 3.1 implies that

$$1 - \alpha \leq \mathbb{P}(Y_{n+1} \in \mathcal{R}_{Z_{n+1}}(X_{n+1}; f_{\bar{\tau}_{n+1}}(Q_\beta\left(\frac{1}{n} \sum_{k=1}^n \delta_{V_k}\right)))) < 1 - \alpha + \frac{1}{n + 1}.$$

Setting $\beta = (1 - \alpha)(1 + n^{-1})$ in the previous inequality and using the definition of $\bar{\mathcal{C}}_\alpha(X_{n+1})$ given in (17) concludes the proof. \square

ADJUSTMENT	Trivial	Linear	Exp	Tanh	Sigmoid
$f_\tau(\lambda)$	λ	$\tau\lambda$	$\exp(\tau\lambda)$	$\tan(\tau\lambda)$	$(1 + \exp(-\lambda\tau))^{-1}$
$f_\tau^{-1}(\lambda)$	λ	$\tau^{-1}\lambda$	$\tau^{-1}\log \lambda$	$\tau^{-1}\arctan \lambda$	$\tau^{-1}\log((1 - \lambda)^{-1}\lambda)$

Table 2: Adjustment Functions f_τ and their inverses f_τ^{-1} .

B Experimental setup and results

This section aims to provide a comprehensive understanding of the CP² algorithm. We want to further explore the CP² approach and to better explain the key concepts.

B.1 Algorithm structure and features

We detail the construction of the prediction sets given by CP². The algorithm is divided into two parts: the first part computes the quantile $Q_{1-\alpha}(\mu)$ (Algorithm 1), and the second part constructs the prediction set $\mathcal{C}_\alpha(x)$ (Algorithm 2).

Algorithm 1 Quantile Computation

Input: dataset $\{(X_k, Y_k)\}_{k \in [n]}$, significance level α , confidence set \mathcal{R} , conditional distributions $\Pi_{Y|X}$ and $\Pi_{Z|X}$, function f_τ .

for $k = 0$ **to** n **do**

Sample $Z_k \sim \Pi_{Z|X=X_k}$

$(\bar{\tau}_k, \bar{\lambda}_k) \leftarrow$ Equations (2) and (3)

Compute $V_k = f_{\bar{\tau}_k}^{-1}(\bar{\lambda}_k)$

Set $k_\alpha = \lceil (1 - \alpha)(n + 1) \rceil$

$V_{(k_\alpha)} \leftarrow$ k_α -th smallest value in $\{V_k\}_{k \in [n]} \cup \{\infty\}$

Output: $V_{(k_\alpha)}$.

Algorithm 2 Prediction Set Computation

Input: new data x , dataset $\{(X_k, Y_k)\}_{k \in [n]}$, significance level α , confidence set \mathcal{R} , conditional distributions $\Pi_{Y|X}$ and $\Pi_{Z|X}$, function f_τ .

$Q_{1-\alpha}(\mu) \leftarrow$ Algorithm 1

Sample $z \sim \Pi_{Z|X=x}$

$\tau_{x,z} \leftarrow$ Equations (2) and (3)

Output: $\mathcal{R}_z(x; f_{\tau_{x,z}}(Q_{1-\alpha}(\mu)))$.

Choice of f_τ . We present examples of mappings f_τ and their inverses f_τ^{-1} in Table 2. The choice of the mapping f_τ is crucial for the performance of the method, and we investigate their impact in Section 4. For instance, choosing $f_\tau(\lambda) = \tau\lambda$ results in conditionally valid prediction sets, as long as $\Pi_{Y|X=x}$ accurately estimates the conditional distribution $P_{Y|X=x}$; see Corollary 3.3.

B.2 Details of the experimental setup

We use the Mixture Density Network [4] implementation from CDE [33] Python package ¹ as a base model for CP, PCP and CP². The underlying neural network contains two hidden layers of 100 neurons each and was trained for 1000 epochs for each split of the data. Number of components of the Gaussian Mixture was set to 10 for all datasets.

For the CQR [30] and CHR [35] we use the original authors' implementation ². The underlying neural network that outputs conditional quantiles consists of two hidden layers with 64 neurons each. Training was performed for 200 epochs for batch size 250.

We replicate the experiments for 50 random splits of all nine datasets. To lower noise in calculated performance metrics we reuse trained networks and samples across different top-level algorithms for each replication.

¹https://github.com/freelunchtheorem/Conditional_Density_Estimation

²<https://github.com/msesia/chr>

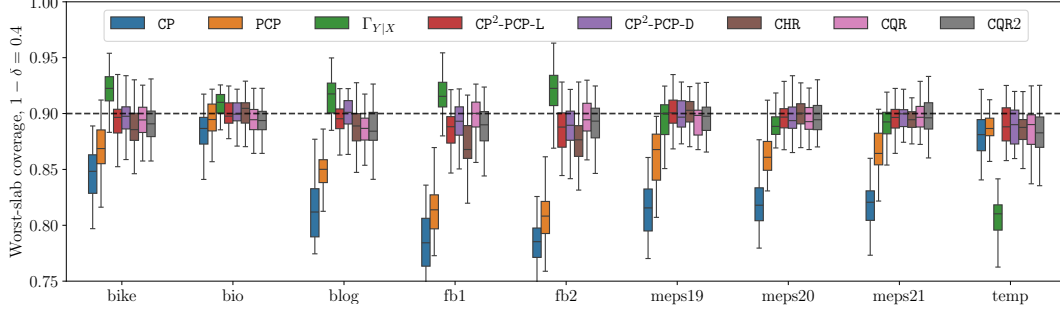


Figure 8: Worst-slab coverage on real data, $(1 - \delta) = 0.4$.

B.3 Worst-slab coverage

Here we present some additional experiments related to conditional coverage achieved by different methods. We have used Worst Slab Coverage metric, which is sensitive to the set of labs considered during the search. Following [8, 31], recall that a slab is defined as

$$S_{v,a,b} = \{x \in \mathbb{R}^p : a < v^T x < b\},$$

where $v \in \mathbb{R}^p$ and $a, b \in \mathbb{R}$, such that $a < b$. Now, given the prediction set $\mathcal{C}(x)$ and $\delta \in [0, 1]$, the *worst-slab coverage* is defined as:

$$\text{WSC}(\mathcal{C}, \delta) = \inf_{v \in \mathbb{R}^p, a < b \in \mathbb{R}} \mathbb{P}(Y \in \mathcal{C}(X) | X \in S_{v,a,b}) \text{ s.t. } \mathbb{P}(X \in S_{v,a,b}) \geq 1 - \delta.$$

In Section 4, we presented the results obtained for $(1 - \delta) = 0.1$. In this case, the considered slabs must contain at least 10% of the data. In Figure 8 we report results obtained for $(1 - \delta) = 0.4$. We can see that performance improves a lot compared to $\delta = 0.1$, and most results become indistinguishable.

B.4 Extended results of real data experiments

Table 3 we summarize all metrics from our real-world data experiments. For conditional coverage we report worst-slab coverage with $(1 - \delta) = 0.1$. On six out of nine datasets CP^2 method achieves the best result in conditional coverage.

B.5 Other perspective on conditional coverage

The worst-slab coverage metric used in the previous section is not always helpful: (1) it provides a single number for each method, and (2) the selected slab is different for each algorithm. In practice we might be interested in how sharp the coverage is along the portion of the input space spanned by the test data. To explore this, we used two approaches: dimensionality reduction and clustering. Results for clustering with HDBSCAN are presented in the main part in Figure 7, here turn to dimensionality reduction.

First we apply UMAP algorithm to project data to two dimensions and then construct a heatmap plot to show coverage in each bin of the histogram. Results for meps_19 dataset are presented in Figure 9. Nominal coverage is set to $(1 - \alpha) = 0.9$ and corresponds to gray part of the color scale. We can see that our method and baseline $\Pi_{Y|X}$ perform better than CP and PCP across the space.

C Further discussion on the method

In this section, we address the limitations of CP^2 . This general framework was designed to combine the advantages of both frequentist and Bayesian methods. The CP^2 method can create a broad range of methods by combining f_τ and Π_x alongside existing conformal techniques.

Table 3: Real data experiments: M. Cov. stands for marginal coverage, C. Cov. is worst-slab coverage (here $(1 - \delta) = 0.4$) and w_{sd} is average total length of the prediction sets, scaled by standard deviation of Y . Nominal coverage level is set to $(1 - \alpha) = 0.9$. For $\Pi_{Y|X}$, PCP, CP^2 -PCP we use the same underlying mixture density network model with 50 samples. CHR and CQR(2) also share the same base neural network model. We average results of 50 random data splits. For each dataset, we highlighted the algorithm achieving the closest conditional coverage.

Dataset	Metric	CP	PCP	$\Pi_{Y X}$	CP^2 -PCP-L	CP^2 -PCP-D	CHR	CQR	CQR2
bike	M. Cov.	0.90	0.90	0.93	0.90	0.90	0.90	0.90	0.90
	C. Cov.	0.79	0.85	0.92	0.90	0.90	0.88	0.89	0.88
	w_{sd}	0.71	0.71	0.83	0.77	0.81	1.93	2.21	2.27
bio	M. Cov.	0.90	0.90	0.91	0.90	0.90	0.90	0.90	0.90
	C. Cov.	0.88	0.89	0.91	0.90	0.90	0.90	0.88	0.89
	w_{sd}	2.34	1.89	1.95	1.89	1.91	1.92	2.13	2.10
blog	M. Cov.	0.90	0.90	0.91	0.90	0.90	0.90	0.90	0.90
	C. Cov.	0.60	0.74	0.91	0.89	0.90	0.88	0.88	0.87
	w_{sd}	0.60	0.30	0.72	0.60	0.71	0.31	0.42	0.39
fb1	M. Cov.	0.90	0.90	0.93	0.90	0.90	0.90	0.90	0.90
	C. Cov.	0.49	0.64	0.92	0.88	0.89	0.86	0.89	0.88
	w_{sd}	0.47	0.28	0.58	0.49	0.58	0.28	0.39	0.35
fb2	M. Cov.	0.90	0.90	0.93	0.90	0.90	0.90	0.90	0.90
	C. Cov.	0.50	0.61	0.91	0.87	0.88	0.87	0.89	0.88
	w_{sd}	0.53	0.32	0.65	0.53	0.65	0.32	0.41	0.36
meps19	M. Cov.	0.90	0.90	0.89	0.90	0.90	0.90	0.90	0.90
	C. Cov.	0.54	0.78	0.89	0.90	0.90	0.90	0.89	0.89
	w_{sd}	1.05	0.73	1.02	1.06	1.04	0.76	1.09	1.17
meps20	M. Cov.	0.90	0.90	0.89	0.90	0.90	0.90	0.90	0.90
	C. Cov.	0.58	0.80	0.89	0.89	0.89	0.90	0.89	0.90
	w_{sd}	1.06	0.75	0.98	1.02	1.00	0.76	1.08	1.16
meps21	M. Cov.	0.90	0.90	0.89	0.90	0.90	0.90	0.90	0.90
	C. Cov.	0.54	0.81	0.89	0.90	0.90	0.90	0.89	0.89
	w_{sd}	1.04	0.72	0.99	1.04	1.01	0.76	1.13	1.20
temp	M. Cov.	0.90	0.90	0.82	0.90	0.90	0.90	0.90	0.90
	C. Cov.	0.87	0.89	0.81	0.89	0.88	0.87	0.86	0.87
	w_{sd}	0.87	0.92	0.78	0.94	0.93	1.32	1.48	1.30

However, it is important to recognize that our method has its own challenges. Specifically, it relies on an estimator for the conditional distribution $P_{Y|X}$, which may be difficult to obtain in certain real-world situations. Additionally, our approach might not be compatible with all conformal methods, like with binning procedures.

Our theoretical analysis of the conditional validity illustrates the benefit of more adaptive strategies. These findings may prove helpful to improve the empirical performance of conformal prediction in various problems.

We are excited about the potential of our work to contribute to the development of new uncertainty management techniques. Specifically, when it comes to refining confidence regions obtained via Bayesian methods.

In summary, our results showcase the promise of CP^2 in improving the reliability of machine learning models. We hope that our research will motivate further progress in this field and inspire researchers to explore the vast possibilities of this approach.

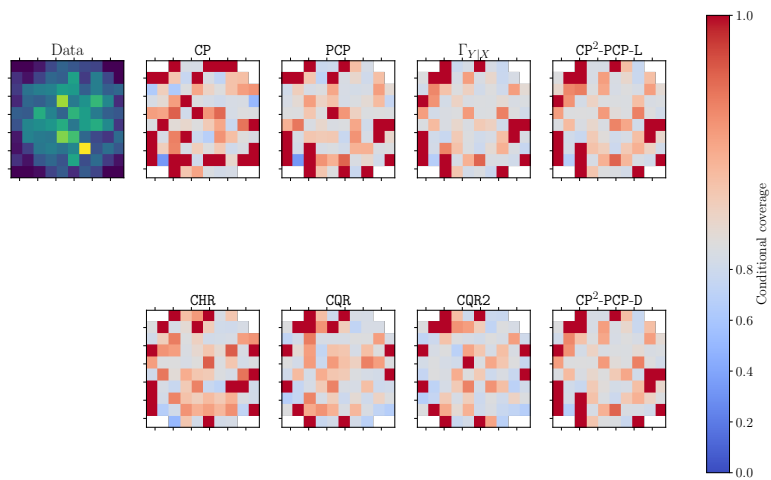


Figure 9: Conditional coverage after dimensionality reduction, `meps_21` dataset. Data projected to two dimensions using UMAP algorithm with Canberra metric, with the `n_neighbors` hyperparameter set to 2. Nominal coverage is set to $(1 - \alpha) = 0.1$, it corresponds to gray on the color scale.

Table 4: Summary results of experiments on real data: New version. M. Cov. stands for marginal coverage, C. Cov. is worst-slab coverage (here $(1 - \delta) = 0.1$) and w_{sd} is average total length of the prediction sets, scaled by standard deviation of Y . Nominal coverage level is set to $(1 - \alpha) = 0.9$. For $\Pi_{Y|X}$, PCP, CP^2 -PCP we use the same underlying mixture density network model with 50 samples. CHR and CQR(2) also share the same base neural network model. We average results of 50 random data splits. For each dataset, we highlighted the algorithm achieving the closest conditional coverage.

Dataset	Metric	$\Pi_{Y X}$	CP^2				CHR	CP	CQR	CQR2	PCP
			HYB-D	HYB-L	PCP-D	PCP-L					
bike	M. Cov.	0.93	0.90	0.90	0.90	0.90	0.90	0.90	0.90	0.90	0.90
	C. Cov.	0.92	0.90	0.90	0.89	0.89	0.88	0.79	0.90	0.87	0.85
	w_{sd}	0.83	0.81	0.77	0.80	0.79	1.94	0.71	2.25	2.31	0.71
bio	M. Cov.	0.91	0.90	0.90	0.90	0.90	0.90	0.90	0.90	0.90	0.90
	C. Cov.	0.91	0.90	0.90	0.90	0.90	0.90	0.88	0.89	0.89	0.89
	w_{sd}	1.95	1.91	1.89	1.95	1.97	1.92	2.34	2.13	2.10	1.89
blog	M. Cov.	0.91	0.90	0.90	0.90	0.90	0.90	0.90	0.90	0.90	0.90
	C. Cov.	0.91	0.90	0.89	0.90	0.89	0.87	0.60	0.87	0.86	0.74
	w_{sd}	0.72	0.71	0.60	0.71	0.72	0.31	0.60	0.44	0.39	0.30
fb1	M. Cov.	0.93	0.90	0.90	0.90	0.90	0.90	0.90	0.90	0.90	0.90
	C. Cov.	0.92	0.89	0.88	0.89	0.88	0.87	0.49	0.90	0.87	0.64
	w_{sd}	0.58	0.58	0.49	0.59	0.56	0.26	0.47	0.37	0.33	0.28
fb2	M. Cov.	0.93	0.90	0.90	0.90	0.90	0.90	0.90	0.90	0.90	0.90
	C. Cov.	0.91	0.88	0.87	0.88	0.88	0.88	0.50	0.89	0.89	0.61
	w_{sd}	0.65	0.65	0.53	0.65	0.62	0.33	0.53	0.43	0.37	0.32
meps19	M. Cov.	0.89	0.90	0.90	0.90	0.90	0.90	0.90	0.89	0.90	0.90
	C. Cov.	0.89	0.90	0.90	0.89	0.90	0.90	0.54	0.88	0.89	0.78
	w_{sd}	1.02	1.04	1.06	1.07	1.19	0.76	1.05	1.14	1.19	0.73
meps20	M. Cov.	0.89	0.90	0.90	0.90	0.90	0.90	0.90	0.90	0.90	0.90
	C. Cov.	0.89	0.89	0.89	0.90	0.90	0.91	0.58	0.88	0.89	0.80
	w_{sd}	0.98	1.00	1.02	1.04	1.15	0.77	1.06	1.09	1.17	0.75
meps21	M. Cov.	0.89	0.90	0.90	0.90	0.90	0.90	0.90	0.90	0.90	0.90
	C. Cov.	0.89	0.90	0.90	0.89	0.89	0.90	0.54	0.89	0.88	0.81
	w_{sd}	0.99	1.01	1.04	1.04	1.16	0.79	1.04	1.13	1.21	0.72
temp	M. Cov.	0.82	0.90	0.90	0.90	0.90	0.90	0.90	0.90	0.90	0.90
	C. Cov.	0.81	0.88	0.89	0.89	0.88	0.86	0.87	0.85	0.86	0.89
	w_{sd}	0.78	0.93	0.94	0.93	0.96	1.31	0.87	1.48	1.30	0.92